Lytic/Lysogenic Transition as a Life-History Switch

Joan Roughgarden[1 2]

November 27, 2023

Abstract

The transition between lytic and lysogenic life cycles is the most important feature of the life history of temperate viruses. An optimal life-history explanation for this transition is offered based a discrete-time model of phage/bacteria population dynamics featuring infection of bacteria by Poisson sampling of virions from the environment. The time step is the viral latency period. In this model density-dependent viral absorption onto the bacterial surface is sufficient to produce virus/bacteria coexistence and density-dependence in bacterial growth is not needed.

The formula for the transition between lytic and lysogenic phases is termed the "fitness switch". According to the model, the virus switches from lytic to lysogenic when its population grows faster as prophage than as virions produced by lysis of the infected cells, and conversely for the switch from lysogenic to lytic.

A prophage that benefits the bacterium it infects automatically incurs lower fitness upon exiting the bacterial genome, resulting in its becoming locked into the bacterial genome in what is termed here as a "prophage lock".

The fitness switch qualitatively predicts the ecogeographic rule that environmental enrichment leads to microbialization with a concomitant increase in lysogeny, fluctuating environmental conditions promote virus-mediated horizontal gene transfer, and prophage-containing bacteria can integrate into the microbiome of a eukaryotic host forming a functionally integrated tripartite holobiont. These predictions accord more with the "Piggyback-the-Winner" hypothesis than with the "Kill-the-Winner" hypothesis in virus ecology.

Introduction

Viruses have enormous ecological impact (Suttle 2007, Youle *et al.* 2012, O'Malley 2016). Marine viruses infect approximately 10^{23} bacterias every second, removing 20%–40% of the standing stock of marine bacterias each day (Suttle 2007). They are able to exert top-down control of marine microbial abundance comparable to that of zooplankton grazing, thereby affecting marine food webs and biogeochemical cycles (Breitbart *et al.* 2018). Furthermore, viruses represent 94% of the nucleic-acid-containing particles in the oceans (Breitbart *et al.* 2018). Hence, virus also

[1]Hawaii Institute of Marine Biology, University of Hawaii, joaner@hawaii.edu and Department of Biology, Stanford University, rough@stanford.edu, ORCID: https://orcid.org/0000-0002-6360-7964.

[2]Keywords: bacteriophage, phage, holobiont, hologenome, lytic, lysogenic, life-history, fitness switch, microbialization, ecogeographic rules, viral biogeography, prophage lock, horizontal gene transfer, tripartite holobiont, piggyback-the-winner, kill-the-winner, mathematical model, population dynamics.

represent an enormous number of evolutionary agents whose phenotypes are shaped by natural selection.

The most important feature of the life history of temperate viruses is their transition between lytic and lysogenic strategies, that is, from a strategy in which a virus infects a bacterium, commandeers its reproductive machinery to produce new viruses and then kills the infected bacterium when releasing the newly minted viruses into the environment *vs.* a strategy of incorporating into the bacteria's genome as a "prophage" and reproducing along with the bacterium itself. Lytic virus are particularly important for food web dynamics and biogeochemical cycles because "lysis", that is, the breakdown of the bacterial cell wall, allows the contents of bacterial cells to spill into the media as dissolved organic matter (DOM). As a result, the carbon in infected bacterial cells is intercepted on its journey up the food web—this interception is called the "viral shunt" (Suttle 2007). The viral shunt contrasts with zooplankton grazing on bacteria whereby carbon is passed up the food web when the zooplankton are themselves preyed upon. Thus, which strategy the virus adopts greatly influences its ecological impact. It is lytic viruses that cause bacterial mortality along with the viral shunt, whereas lysogenic viruses do not cause bacterial mortality or a viral shunt. Furthermore, prophages often carry extra genes not pertaining to virus's own replication but that are expressed by the infected bacterium along with the bacteria's own genes. These extra genes supplied by the prophage may benefit the bacterium, for example, by endowing it with resistance to antibiotics or by producing pathogenicity to would-be grazers. The virus is a symbiont that can be thought of as a commensal or mutualist when existing as a prophage or as a parasite when existing in the lytic phase. Therefore, determining the evolutionary basis for a switch between lytic and lysogenic life history strategies is of inherent evolutionary interest from life-history and symbiosis perspectives and has great ecological significance as well.

Previous models for the lytic/lysogenic switch (Santillán and Mackey 2004, Ding and Lao 2009, Bednarz *et al.* 2014, Mackey *et al.* 2016, Ch. 7, Sinha *et al.* 2017, Cheong *et al.* 2022, Shivam *et al.* 2022) offer mechanistic accounts of the molecular regulatory network for the switch, feature systems of nonlinear delay-differential equations, assume mass action collision as the mechanism of viral colonization of the host and postulate density-dependent bacterial population growth.

Instead, this paper draws on the approach in Ecology pertaining to life-history switches such as those between vegetative growth and flowering in annual plants and between tadpole and adult phases in amphibians *etc*. (*cf.* Schaffer 1983). Models of these developmental switches rely on some equation relating fitness to the time of switching. Then the optimal switch time is computed as that maximizing fitness. Here, the switch is between different life cycles rather than different developmental stages. Still, the idea is the same. The transition between lytic and lysogenic life cycles can be found as the boundary between situations in which one or the other life cycle yields the highest fitness.

To develop a formula to predict the conditions for the lytic/lysogenic switch this paper introduces a new model for virus/bacteria population dynamics. This paper's model differs from previous virus/bacteria population models in being simpler, boiling down to one equation, and uses different assumptions, namely, viral colonization of the host as a Poisson process rather than by mass-action collisions, density independent rather than density dependent bacterial population growth, and it avoids delay-differential equations by taking the viral latency period as the time step in a discrete-time equation analogous to the generation time in population-genetic models.

The new model reveals the conditions for virulent phage and bacteria to coexist as well as the conditions for temperate phage to switch from a lytic to lysogenic life cycle and back again. The mathematical formula for the switch is termed the "fitness switch." The qualitative implications of the fitness switch for the process of virus-mediated horizontal gene transfer (HGT, transduction), for the formation of three-level holobionts consisting of virus, bacteria and host, as well as for various ecogeographic patterns in viral biogeography are developed.

The terminology used in the phage/bacteria interaction is summarized in the Supplementary Material. A critique of models using delay-differential equations, mass-action colonization, and density-dependent bacterial population growth is also included in the Supplementary Material.

The model pertains initially to virulent phage that are permanently lytic and then to temperate phage that allow switching between lytic and lysogenic life cycles.

Virulent Phage: Virus/Bacteria Population Dynamics

Figure 1 (Left) offers a diagram of a virulent virus/bacteria life cycle for a system of equations describing virus and bacteria population dynamics. The model is defined in discrete time with the time step being the viral latency period. A time step begins with the state variables, $N(t)$ and $V(t)$ for the number of bacteria and free virus particles (virions) in their environmental source pools at time t. Then the virus infect the uninfected bacteria according to a Poisson distribution such that some bacteria remain uninfected, some have only one infection, some have two infections *etc*. (Ellis and Delbrück 1939). Poisson searching for hosts was featured in early parasitoid/host models (Nicholson and Bailey 1935) and more recently for bacterial colonization of hosts in Roughgarden (2018, 2020, 2023).

The Poisson distribution describing the infection process has density parameter, $\mu(t) \equiv a(v(t))\, v(t)$ where $v(t) \equiv V(t)/N(t)$ is the ratio of virus to bacteria in their source pools. The $a(v(t))$ is the adsorption function—it refers to the probability that a viral particle comes in contact with a bacterium and binds to surface molecules for subsequent incorporation into the bacterial cell. Adsorption is a function of $v(t)$ because the number binding sites on the surface of the bacterium is finite and the sites may become saturated. Thus, $a(v(t))$ includes information about the

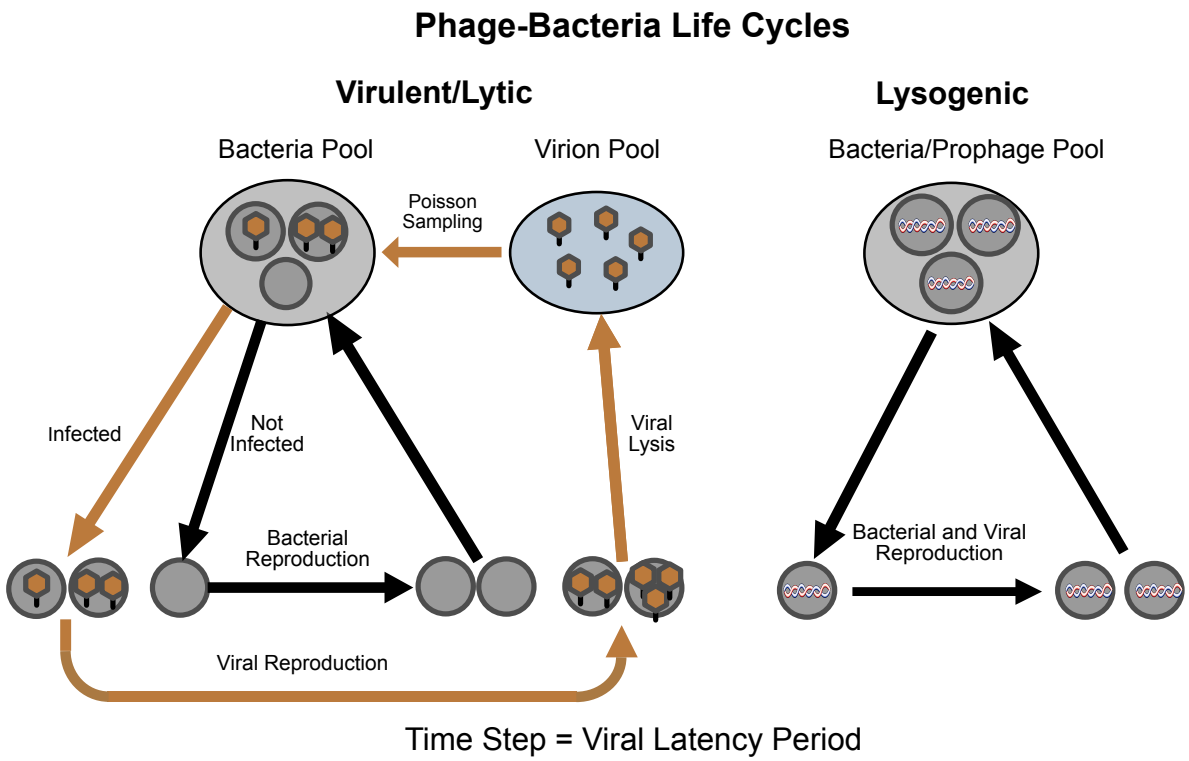

Figure 1: *Phage/bacteria life cycles. Left: life cycle for virulent phages and for the lytic phase of temperate phages. Bacteria in the bacterial source pool in the environment are infected by free virus particles (virions) from the viral source pool according Poisson sampling. The infected bacteria are the site of viral replication, leading to the release of new virions and the death of the infected cells. The uninfected bacteria replicate to produce more bacteria available for infection to begin the next time step. Right: life cycle for the lysogenic phase of temperate phages. The virus is represented as a helix that is incorporated as a prophage into the genome of its bacterial host. The virus life cycle is coincident with the bacterial life cycle. The time step is the viral latency period.*

binding affinity of virus particles to receptors in the bacterial surface and also about the number of binding sites. Furthermore, $a(v(t))$ also includes information about the accessibility of the bacterium to virus particles and has a role similar to the colonization parameter, d in a model for bacteria colonization of a host to form a holobiont (Roughgarden 2023). For a given ratio of virus to bacteria, $v(t)$, if the environment is such that virus are prevented from reaching the bacteria, then $a(v(t))$ is low compared to $a(v(t))$ in environments that allow ready access of the virus to the bacteria. Environments may differ in how viscous the media is, or for airborne virus particles, whether air filters are installed.

Recursion Equations in Discrete Time

According to a Poisson distribution, the fraction of uninfected bacteria that remain uninfected, $P_0(\mu(t))$, is $e^{-\mu(t)}$ and the fraction of bacteria colonized by m virus, $P_m(\mu(t))$, is $\frac{e^{-\mu(t)}\mu(t)^m}{m!}$ for $m \geq 0$ where $\mu(t) = a(v(t))\, v(t)$. The m indexes the number of virus per bacterium. The fraction of bacteria that are infected by one or more virus is $1 - P_0(\mu(t))$.

The uninfected bacteria population increases by a geometric factor of increase per time step, R. Necessarily, $R > 1$, for the bacteria to be able to increase in the absence of the virus. Accordingly, the uninfected bacteria resupply the bacterial source pool as

$$N(t+1) = R\, P_0(\mu(t))\, N(t) \tag{1}$$

where $P_0(\mu(t))$ is the Poisson probability that a bacterium is uninfected.

Next, the virus in the infected bacteria produce new virus particles as

$$\begin{aligned} V(t+1) &= \Big(b(1)\, P_1(\mu(t)) + b(2) P_2(\mu(t)) + \dots\Big)\, N(t) \\ &= \Big(\sum_{m=1}^{\infty} b(m)\, P_m(\mu(t))\Big)\, N(t) \end{aligned} \tag{2}$$

where $b(m)$ is the burst size from a bacterium infected with m virus particles and $P_m(\mu(t))$ is the Poisson probability that a bacterium is infected by m virus particles. More succinctly,

$$V(t+1) = \widetilde{b}(\mu(t))\, N(t) \tag{3}$$

where

$$\widetilde{b}(\mu(t)) \equiv \sum_{m=1}^{\infty} b(m)\, P_m(\mu(t)) \tag{4}$$

and $\widetilde{b}(\mu(t))$ is the burst per bacterium from all the infected bacteria at time t.

Eqs. 1 and 2 together constitute a population-dynamic model for virulent virus and bacteria populations based on the life cycle sketched in Figure 1 (Left). The parameters in the model are R, the geometric factor of increase for uninfected bacteria, $a(v)$, the adsorption function, and $b(m)$, the burst-size function.

The model may be simplified by dividing Eq. 3 by Eq. 1

$$\frac{V(t+1)}{N(t+1)} = \frac{\widetilde{b}(\mu(t))\, N(t)}{R\, P_0(\mu(t))\, N(t)}$$

Then identify $v(t+1)$ with $\frac{V(t+1)}{N(t+1)}$ and $v(t)$ with $\frac{V(t)}{N(t)}$ yielding

$$v(t+1) = \frac{\widetilde{b}(\mu(t))}{R\, P_0(\mu(t))} \tag{5}$$

Equation 5 is a dynamical equation in one variable, $v(t)$, where $\mu(t) = a(v(t))\, v(t)$.

Density dependence in the burst size, $b(m)$, and/or the absorption function, $a(v)$, potentially leads to a stable equilibrium viral to bacteria ratio, $\hat{v}$. The $\hat{v} > 0$ is a necessary condition for stable coexistence of a virulent virus and its host. Alternatively, for some parameter values, $\hat{v} < 0$, indicating that the virus cannot coexist with the host. Still another possibility is that the virus can coexist with the host, $\hat{v} > 0$, but the virus' impact on the host is sufficient to drive the bacteria (and itself) to extinction.

This model does not require an assumption of density-dependent bacterial population growth. The stability, or lack thereof, of virus/bacteria coexistence in this model is determined solely by properties of the virus/bacteria interaction itself as contained in the $b(m)$ and/or $a(v)$ functions. That is to say, the model may be thought of as pertaining to the log phase of bacterial population growth. Once a stable virus/bacteria equilibrium ratio is reached during the bacterial log phase, both parties possess a common geometric growth factor. Then, external to the virus/bacteria interaction, density dependent might *also* occur in the bacterial population dynamics, *e.g.*, the bacteria might grow according to a logistic equation. If so, after attaining coexistence at a stable virus/bacteria ratio during their log phase, the population pair can proceed to grow together with their common geometric growth factor eventually reaching a joint stationary phase determined in part by the microbial carrying capacity.

This qualitative picture of virus/bacteria population dynamics is fundamentally different from the classical picture proposed in Campbell (1961) and later. The Campbell model envisions that virus/bacteria population dynamics involves two counteracting forces—the stabilizing force of density-dependent bacterial population growth and the destabilizing force of time lags arising from the virus latency period. The outcome is a balance of these forces. Accordingly, the formulas for the virus/bacteria equilibrium and its stability in the Campbell model depend on value of the microbial carrying capacity as well as on parameters pertaining to the virus/bacteria interaction. This commingling of parameters for the virus/bacteria interaction with those for bacterial population growth leads to peculiar predictions.

For example, according to the formula for the equilibrium in the Campbell model (*cf.* Eq. S6), small mammals should have fewer phage infecting bacteria than large mammals because the low bacterial carrying capacity in their small guts precludes the coexistence of many types of phage. Conversely, large mammals should support more phage infecting their bacteria because the large carrying capacity for bacteria in their large guts allows more types of phage to coexist with bacteria. However, this phage/bacteria coexistence in large mammals may be temporary because the weakened density dependence from a large bacterial carrying capacity should lead to large virus/bacteria oscillations. No evidence supports this qualitative picture.

The question of which qualitative picture applies to the phage/bacteria interaction, namely that offered by the present model *vs.* that offered by the classical model of Campbell (1961), will ultimately need to be settled empirically. In the meantime, a comparison of the models might

Table 1: Example Parameters in Model

Time Step	15 min
R	2
b_o	40
a_o	0.1
κ	2 to 20, Increment 2

be assisted by the Supplementary Material that offers a detailed mathematical summary of the Campbell (1961) model as well as discussion of its quantitative and technical limitations.

Turning now to the present model, density dependence in burst size might, in principle, underwrite stable coexistence of virus and bacteria. However, the evidence shows that density dependence in burst size is weak (*cf.* Gadagkar and Gopinathan 1980, Figs. 4–5, Patel and Rao 1984, Fig. 1–2). Using these published data relating burst size to m, analysis in the Supplementary Material shows that density dependence in burst size does not allow for stable virus/bacterial coexistence. In contrast, it will be shown here that density dependence in viral absorption onto the bacterial surface does allow stable virus/bacteria coexistence.

The molecular biology of viral absorption onto the surface of bacterial and animal cells has been the focus of much recent study (Dimitrov 2004, Grove and Marsh 2011, Yamauchi and Helenius 2013, Maginnis 2018, Koehler *et al.* 2020, Huss *et al.* 2021). The kinetics of virus binding to cell surface has also been investigated (Moldovan *et al.* 2007, Hubbs *et al.* 2019, Echeverría-Vega *et al.* 2020, Koonjan *et al.* 2022). These studies do not present data directly on $a(v)$ but are nonetheless consistent with the assumption that the binding sites for virus on the surface of a bacterium become saturated as the density of viral particles increase. Accordingly, the absorption function will be taken as $a(v(t)) = a_o\,(1 - \frac{v(t)}{\kappa})$ where κ is the saturation density—the viral density at which all the binding sites per bacterium are occupied and a_o is the maximal probability of binding when all the binding sites are available, given the environmental conditions. Also, it is required that $0 \leq v(t) \leq \kappa$. This formula postulates that the probability of a viral particle binding to a bacterium tends to zero as the binding sizes fill up, and equals zero when the viral density, v, equals κ.

Because density-dependent absorption does allow stable virus/bacteria coexistence, subsequent analysis assumes solely density-dependent absorption without any density dependence in burst size.

Density-Dependent Absorption: $a(v(t)) = a_o\,(1 - \frac{v(t)}{\kappa})$, $b(m) = b_o\,m$

Here,

$$\mu(t) = a_o\,(1 - \frac{v(t)}{\kappa})\,v(t) \tag{6}$$

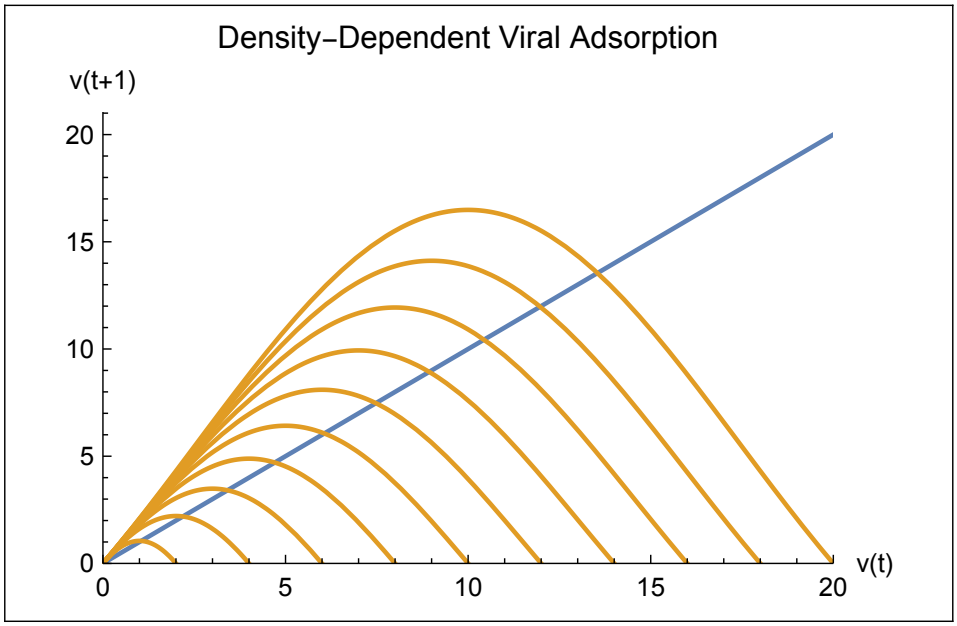

Figure 2: *$v(t+1)$ vs. $v(t)$, in brown, for density-dependent absorption from Eq. 8. The diagonal line, in blue, indicates $v(t+1) = v(t)$. The intersection of the brown curve with the blue line indicates an equilibrium point where virus and bacteria coexist provided the equilibrium is stable. Here, $a_o = 0.1$, $b_o = 40$, $R = 2$, and κ varies left to right from 2 to 20 in steps of 2.*

and, upon doing the summation in Eq. 4[3],

$$\widetilde{b}(\mu(t)) = b_o\, a_o\, (1 - \frac{v(t)}{\kappa})\, v(t) \tag{7}$$

so Eq. 5 becomes

$$v(t+1) = \frac{b_o}{R}\, \frac{a_o\, (1 - \frac{v(t)}{\kappa})\, v(t)}{e^{-a_o\, (1 - \frac{v(t)}{\kappa})\, v(t)}} \tag{8}$$

Illustrative parameter values roughly follow those used in the Supplementary Material for the Campbell (1961) model. The time step, which is the latency period, is 15 minutes, implying four steps per hour. Using the Campbell value for r would lead to a geometric factor of bacterial population growth per time step, R, of 2.68 *i.e.* $(1 + e^{0.0347 \times 15})$. For simplicity, R is taken as 2. The per-virus burst size, b_o, is taken as 40. The base viral absorption coefficient, a_o is arbitrarily taken as 0.1. For the case with density-dependent absorption, κ is arbitrarily taken as 2 to 20 with a increment of 2. These parameters are summarized in Table 1.

Figure 2 shows the curve for $v(t+1)$ from Eq. 8 and the line for $v(t+1) = v(t)$ for several values of the saturation density κ based on the parameter values in Table 1. The curves intersects the line indicating equilibrium points, $\hat{v}$, at which virus and bacteria can coexist, providing the

[3] *cf.* Poisson summation identities in Supplementary Material

equilibrium points are stable, as analyzed further in the next sections. The equilibrium points, $\hat{v}$, increase with increasing saturation densities, κ. Moreover, the slope of the $v(t+1)$ curve at the intersection point is always negative and become steeper as κ increases.

Condition for Viral Increase when Rare.

The virus population can begin to infect the bacterial population if it can increase when rare. That is, if $v(t) \approx 0$, then $v(t+1) > v(t)$ if

$$v(t+1) = \lambda_0 \, v(t) \tag{9}$$

where

$$\lambda_0 = \frac{d\, v(t+1)}{d\, v(t)}\Big|_{v(t)=0} \tag{10}$$

The λ_0 works out to be

$$\lambda_0 = \frac{a_o \, b_o}{R} \tag{11}$$

The λ_0 must be greater than 1 for the virus to increase when rare, according to Eq. 9. Now, $R > 1$ is the condition for the bacteria to increase in the absence of the virus, which is greater than one by assumption. Therefore, if $a_o \, b_o > R > 1$ the virus can spread into a population of increasing bacteria. This condition means that the absorption probability times the burst size, which is the viral production per time step, must exceed the bacterial production per time step for the virus to spread when rare. Otherwise, the bacteria population outgrows the virus population—the virus cannot keep up.

Given b_o, and R, then Eq. 11 implies that the absorption probability must exceed a minimum for the virus to spread. Putting $\lambda_0 = 1$ and solving for a_o, yields the minimum probability of absorption that permits the virus to spread,

$$a_{o,\min} = \frac{R}{b_o} \tag{12}$$

In the instance of the parameters in Table 1 where b_o is 40 and R is 2, $a_{o,\min}$ works out to be 0.05. Hence a_o has been taken as 0.1 to be safely above the minimum. Given the burst size and the bacterial growth factor, if the absorption probability is less than $a_{o,\min}$ then the virus cannot spread into a growing population of bacteria.

Equilibrium Viral Density, $\hat{v}$

Given that both the virus and bacteria can increase when rare, they may come to the equilibrium at an intersection between the $v(t+1)$ curve and the $v(t+1) = v(t)$ line, as was illustrated in Figure 2. The point of intersection depends on the saturation density, κ. The **FindRoot[]** function in *Mathematica* is used to calculate the value of $\hat{v}$ at an intersection point. Figure 3 (left) shows the curve of $\hat{v}$ obtain in this way as a function of κ.

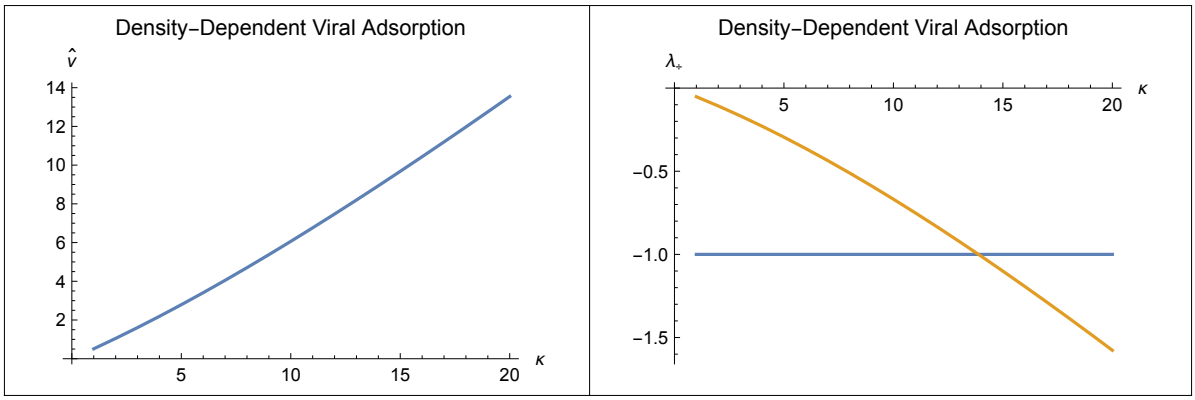

Figure 3: *Left: Equilibrium viral ratio, $\hat{v}$ as a function of κ. Right: Curve is eigenvalue evaluated at $\hat{v}$ as a function of κ and line at -1 marks the boundary between stable and unstable equilibria. The equilibria for κ below 14 are stable and characterized by a damped oscillatory approach whereas the equilibria for κ above 14 are unstable. Here, $a_o = 0.1$, $b_o = 40$, $R = 2$, and κ varies from 1 to 20.*

Stability of $\hat{v}$

The stability of an equilibrium viral ratio, $\hat{v}$, depends on λ_+ defined as

$$\lambda_+ = \frac{d\,v(t+1)}{d\,v(t)}\Big|_{v(t)=\hat{v}} \tag{13}$$

The λ_+ is the eigenvalue evaluated at a positive equilibrium point. If λ_+ is between $+1$ and -1 then the equilibrium is stable (*e.g.* Roughgarden 1996). Specifically, if λ_+ is between $+1$ and 0, the approach to equilibrium does not involve oscillations whereas if λ_+ is between -1 and 0, the approach to equilibrium involves damped oscillations.

Figure 3 (right) shows the curve of λ_+ as a function of κ. The λ_+ is always negative, so the approach to equilibrium is oscillatory. The horizontal line at -1 marks the boundary between stable and unstable equilibria. The horizontal line crosses the curve for λ_+ near $\kappa = 14$. Hence, the equilibria, $\hat{v}$, for $\kappa < 14$ are stable with an oscillatory approach. The equilibria for $\kappa > 14$ are unstable.

An additional source of density dependence may smooth the approach to equilibrium. Indeed, if density dependence in burst size is combined with the density dependence in absorption, then the eigenvalue may lie between 0 and $+1$, indicating a non-oscillatory approach to the equilibrium (not shown).

Trajectories

Figure 4 illustrates trajectories of both virus and bacteria for $\kappa < 14$. Trajectories illustrate the damped oscillations of $v(t)$ during the approach to a stable equilibrium. The trajectory of $N(t)$ also shows damped oscillations during the approach to the asymptotic growth factor, although

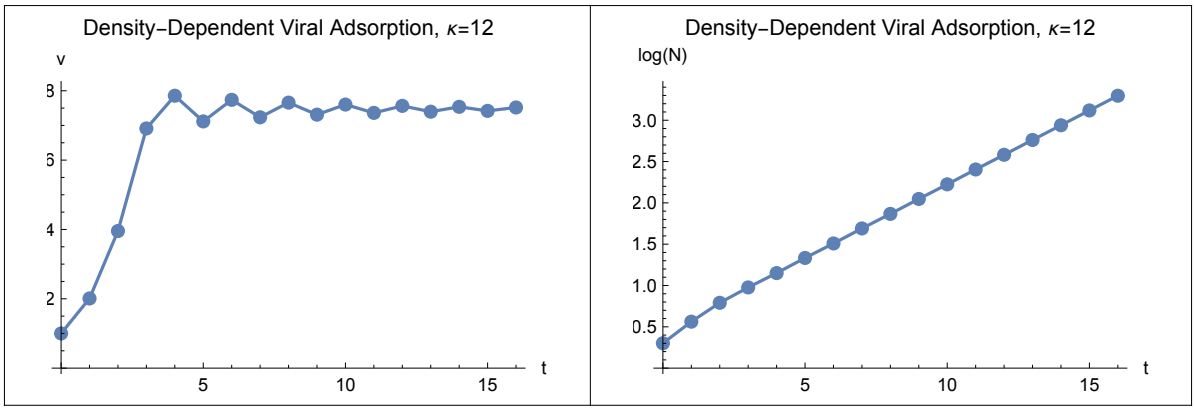

Figure 4: *Left: Trajectory of $v(t)$ showing damped oscillation during approach to equilibrium. Right: Trajectory of $\log_{10}(N(t))$ showing approach to exponential bacterial population growth. Here, $\kappa = 12$, $v(0) = 1$, $N(0) = 2$, $t_{\max} = 16$, $\kappa = 12$, $a_o = 0.1$, $b_o = 40$, $R = 2$ and $t_{\max} = 16$.*

the scale on the graph makes the oscillations difficult to see. The Supplementary Material also includes an illustration of trajectories around an unstable equilibrium where $\kappa > 14$.

Infection Discount

Figure 4 shows the bacterial population increasing with time. However, unlike this figure, the bacterial population does not necessarily increase even though the virus to bacteria ratio has reached a stable equilibrium, $\hat{v}$.

The net growth factor, R', for the bacteria per time step from Eq. 9 is $R' \equiv R\, e^{-\mu(t)}$. The R' must be > 1 for the bacterial population to increase. If the virus to bacteria ratio is at equilibrium, $\hat{v}$, then $\mu(t) = a_o\,(1 - \hat{v}/\kappa)\,\hat{v}$. In this situation,

$$R' = R\, e^{-a_o\,(1-\hat{v}/\kappa)\,\hat{v}} \tag{14}$$

Define the "infection discount", $I(R)$, as

$$I(R) \equiv e^{-a_o\,(1-\hat{v}/\kappa)\,\hat{v}} \tag{15}$$

The infection discount indicates the degree to which the bacterial population growth factor is discounted as a result of the mortality caused by viral infections. The infection discount depends implicitly on R because $\hat{v}$ depends on R along with the other parameters. Hence, the bacteria can increase if

$$R' = R \times I(R) > 1 \tag{16}$$

If $\hat{v} > 0$ and $R' < 1$ then the virus can increase when rare but then subsequently drives the host (and itself) to extinction.

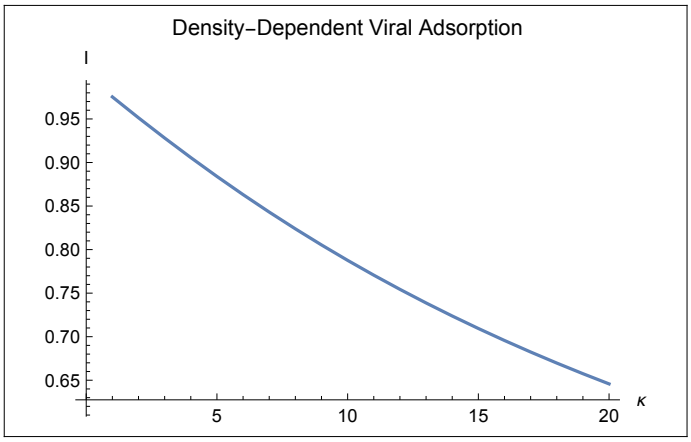

Figure 5: *Infection discount. Here,* $a_o = 0.1$, $b_o = 40$, $R = 2$ *and* κ *varies from 1 to 20.*

Figure 5 illustrates the infection discount for the parameters of Table 1. The discount becomes more severe as κ increases because $\hat{v}$ increases with κ. However, in the table, R is 2 and the discount never drops below $1/2$, so R' remains greater than one even as κ increases to 20. This indicates that the bacterial population can continue to increase for all levels of infection with the parameters of Table 1. Other parameters values (not explored) might not be so kind to the bacterial population.

Temperate Phage: Criterion for Lytic to Lysogenic Transition

The model for the population dynamics of virulent phage in Figure 1 (Left) also applies to the lytic phase of a temperate phage. For the lysogenic phase, a virus incorporates into a bacterium's genome and reproduces along with the bacterium itself as shown in Figure 1 (Right). The main life-history question pertaining to temperate phage is when to transition from lytic to lysogenic and *vice versa*. The premise of this paper is that a phage should switch in the direction that yields it the highest fitness.

The quantitative answer to the lytic/lysogenic life history question follows directly from the condition for virus to increase when rare, Eq. 11. The population dynamics of lysogenic phase is identically the same as that for the bacteria they reside in, namely, increasing by a factor of R each time step. On the other hand, the lytic phase can spread into the population of bacteria if $a_o\, b_o > R$, meaning that the initial absorption probability times the per-virus burst size exceeds the bacterial growth factor. So the lytic phase produces more virus per time step if if $a_o\, b_o > R$ whereas the lysogenic phase produces more virus per time step if $a_o\, b_o < R$. Thus, a "fitness

switch" can be formulated as follows:

$$\begin{aligned} \text{A}: \quad a_o\, b_o &> R \quad - \text{ lytic phase highest fitness for virus} \\ \text{B}: \quad a_o\, b_o &< R \quad - \text{ lysogenic phase highest fitness for virus} \end{aligned} \tag{17}$$

Now consider qualitative predictions of Eq. 17.

Qualitative Predictions of Fitness Switch

Laboratory Conditions

The fitness switch agrees qualitatively with well-known laboratory conditions that cause a lytic/-lysogenic switch. Percent lysogeny in a bacterial host is an increasing function of the number of coinfecting virus (Fry 1959, Kourilsky 1973, Kourilsky and Knapp 1974). The interpretation of this finding according to the fitness switch pertains to competition among the coinfecting virus for the cell's resources. Experimental conditions maintain a constant base absorption, a_o, and bacterial growth factor, R, among treatments but vary in the number of introduced phages. Only the Poisson density, $\mu = a_o\, v$, varies among treatments—this is what leads to varying coinfection among treatments. Furthermore, according to Kourilsky (1973), treatments that depress host macromolecular syntheses favor lysogeny. Hence, one may hypothesize that competition among multiple virus per bacterium affects the number of virons each produces given a limited amount of resources for macromolecular synthesis, thereby lowering the per-virus burst size and making lysogeny adaptive compared with lysis. Even strong density dependence in burst size is not sufficient to stabilize virus/bacteria population dynamics (*cf*. Eq. S17) but density dependent burst size remains relevant to whether an individual virus' fitness is higher *via* the lytic or the lysogenic life cycle. The molecular mechanism underlying an adaptive increase in lysogeny with increasing coinfection might involve an increase in copies of phage repressors of the lytic cycle and of integrase genes needed for entry into the host genome (Silveira *et al*. 2021). This mechanism for attaining increased lysogeny with increased coinfection could be considered as bi-product cooperation among the coinfecting viruses. Active cooperation would be indicated if phage repressor and integrase concentrations exceed what is predicted if these concentrations were to scale linearly with the number of coinfections (*cf*. Kourilsky 1973, Trinh *et al*. 2017).

Conversely, damage to the bacterial DNA, say with ultraviolet iradiation, triggers a so-called SOS response within the bacterium that in turn provokes a prophage to revert to a lytic state, a process called "induction" (Bæk *et al.* 2003). Damage to the bacterial DNA would lead to a lower bacterial R, making lysis adaptive compared with lysogeny.

Beyond the laboratory, the fitness switch is relevant to various environmental scenarios that flip the switch from lytic to lysogenic or *vice versa*.

Intervention Affecting a_o with Hygienic Practice

If the access of virus particles to bacteria is sufficiently lowered by introducing air filters or other hygienic practices, then the best strategy switches from lytic to lysogenic. For example, the minimum value of a_o for the virus to spread in a bacteria population from Eq. 12 using the parameters in Table 1 works out to be 0.05. So if the hygienic practices reduce a_o below 0.05, the the virus should switch from lytic to lysogenic because doing so yields a higher viral population growth. This conclusion is consistent with the conclusion from Stewart and Levin (1984) that "lysogeny is an adaptation for phage to maintain their populations in 'hard times'." In this scenario, the virus are using the bacteria as a refuge.

Environmental Deterioration Affecting b_o and R Simultaneously

If a chemical such as a general toxin, pollutant or antibiotic is introduced into the environment, then whether the virus should switch from lytic to lysogenic depends on the relative impact of the chemical. For example, if the chemical is an antibiotic, then the bacterial growth factor, R, is lowered, say by 50%. Now, the per-virus burst size, b_o is likely affected too because, say, the ATP level and other resources within the bacteria drop, implying that fewer viral particles can be synthesized. If the per-virus burst size is also reduced by 50% as a result, the reductions to both virus and bacteria cancel out in the switch function, Eq. 17, leaving the lytic *vs.* lysogenic state unchanged. But if the chemical sufficiently affects b_o more than R, then the virus could switch from lytic to lysogenic and conversely, if the chemical affects R more than b_o. Thus, the idea of lysygeny offering a refuge for lytic virus to escape "hard times" depends on the relative impact of the deterioration on the virus and on the bacteria.

Viral Biogeography of Lysogeny and Pathogenicity

Several correlations among habitats in the propensity for lysogeny have been discovered. Here is how these patterns might be accounted for based on the fitness switch, Eq. 17.

Microbialization on Coral Reefs—Habitat with High R

Overfishing and eutrophication on coral reefs leads to an increase in fleshy algae. The algae are largely ungrazed and produce an increase in dissolved organic carbon (DOC). The increase in DOC in turn leads to a replacement of the type of bacteria characteristic of low-nutrient environments (oligotrophs) with those typical of nutrient rich environments (copiotrophs). Forest Rohwer and colleagues (Haas *et al.* 2016) refer to this shift in coral reef ecosystem structure as "microbialization." Furthermore, based on 24 coral reefs, they report (Knowles *et al.* 2016) that viromes in microbialized conditions show an increase in the marker genes of temperate viruses, indicating that increased lysogeny accompanies microbialization.

The increase in DOC from microbialization leads to an increase in microbial growth, R. The effect of increasing R in the switch function, Eq. 17, provided that b_o is relatively unchanged, is to switch the virus from lytic to lysogenic, *i.e.* from state A to state B. The fitness switch therefore can predict that the microbialization resulting from increased DOC leads to an increase in lysgenic bacteria, as has been observed.

Rower and colleagues (Haas *et al.* 2016, Silveira *et al.* 2020) further observe that the enrichment of copiotrophs during microbialization is correlated with an increase in virulence genes (Vega Thurber *et al.* 2008). This in turn is correlated with an increase in the prevalence of coral disease (Harvall *et al.* 1999). They conjecture that the pathogenicity of copiotrophs compared with that of oligotriophs is caused by prophages accumulating in the copiotrophs that carry virulence genes for protection of their bacterial hosts. Expression by the bacteria of the virulence genes carried by the prophages produces virulence factors (Bondy-Denomy and Davidson 2014, Davies *et al.* 2016, Obeng *et al.* 2016).

The virulence factors from these genes are of no *direct* value to the virus and its replication within the host, but by assumption, offer protection to their bacterial host. If so, the bacterial R increases because of this increased protection. This increase in R due to the virulence genes being expressed adds to the increase in R caused by the increased DOH that causes microbialization to begin with.

The population growth of the virus as a prophage is identically the same as that for the bacterium, R. So, any assistance the prophage supplies to its bacterial host that increases the bacteria's R identically benefits the prophage as well—no altruism is involved, merely an exact congruence of interests by both the viral prophage and its bacterial host. Thus, the virulence genes are of *indirect* value to the virus that carry them.

Gut Microbiomes—Habitat with High R

The guts of mammals (and presumably other groups too) are sites with concentrated nutrients and food for bacteria, likely increasing the bacterial R beyond that found in the environment while possibly leaving b_o relatively unaffected. As a result, a pattern emerges that parallels that of microbialization, namely, the bacteria of the gut are enriched with prophages, and moreover, those prophages produce virulence and pathogenicity. Specifically, in humans the gut bacteria, *Enterobacterales* and *Bacillales*, harbor significantly higher numbers of prophages and several members of Proteobacteria are the only ones enriched in prophages, compared with other taxonomic groups (López-Leal *et al.* 2022). Similar findings were previously reported for mice (Kim and Bae 2018). Moreover, López-Leal *et al.* 2022) also report that prophages are more abundant in bacteria associated with pathogenic phenotypes agreeing with previous reports, where clinical isolates of *Acinetobacter baumannii* and *Pseudomonas aeruginosa* showed a higher abundance of prophages than environmental isolates (Vallenet *et al.* 2008, Tsao *et al.* 2018). Thus, the *Acinetobac-*

ter and *Pseudomonas* genera were enriched in prophages when these species displayed pathogenic phenotypes. Thus, the pattern of prophage enrichment and increased virulence in gut bacteria appears to share the same explanation as that for coral-reef microbialization because of the high R of bacteria in the gut environment.

Subsurface Ocean—Habitat with Low R and Even Lower $a_o\, b_o$

Bacteria in the middle to deep ocean are enriched with lysogens in contrast to the predominantly lytic lifestyle of their photic-zone counterparts (Mizuno 2016, Luo *et al.* 2020, Yi *et al.* 2023 *cf.* Fig. 1e). Bacterial growth in the deep ocean is very slow with reported doubling times of 1.5 y (Gilgan *et al.* 2020). This pattern contrasts with the increased lysogeny in high-resource fast-growth situations such as eutrophic coral reefs and mammalian guts, as just discussed. Silveira *et al.* (2021) suggest that different mechanisms for coinfection account for these contrasting patterns. Here, an explanation based on the fitness switch, Eq. 17, must postulate that even though the bacterial R is lower in the deep ocean, the product, $a_o \times b_o$, is even lower so that condition B holds. This product may be lower because the micro turbulence at depths with limited wave action might lead to a very low a_o.

Other Habitats With Increased Lysogeny

The prevalence of lysogeny increases with soil depth (Liang *et al.* 2020) and is high in the microbial mats of hot springs characterized by low mobility (Jarett *et al.* 2020).

Collectively, the habitat-lysogeny correlations constitute ecogeographic rules for the biogeography of virus that are logical counterparts of the many ecogeographic rules found in macro ecology. Classic macro ecogeographic rules include the pattern of lower clutch size on islands *vs* the mainland and many others (*cf.* Lomolino 2006, Gaston *et al.* 2008, Baiser *et al.* 2019).

"Prophage Lock"

How long should prophages remain in bacterial genomes before switching back to produce lysis? The fitness switch, Eq. 17, suggests the prophage should remain within their hosts for a long time unless conditions substantially change.

Let the population growth for a bacterium infected with a prophage containing a virulence or other beneficial gene be $R^\star$, where $R^\star > R$, the bacterial growth in the absence of the prophage. Condition B in Eq. 17 then has R replaced by $R^\star$. Because $R^\star > R$, it is more difficult for the virus to switch back to the lytic condition, A, than if it were not carrying a beneficial gene. Thus, once a virus incorporates as a prophage containing a virulence or other gene benefiting the bacteria, it becomes locked into the lysogenic life cycle—it cannot revert back to the lytic life cycle without giving up the $R^\star$ it now enjoys. This situation is termed the "prophage lock."

The possibility that prophages become locked into the lysogenic life cycle because they contain a gene that benefits their bacterial host may explain the longevity of prophages in host genomes through evolutionary time (Hedžet *et al.* 2022) as well as the domestication of prophages (Bobay *et al.* 2014). Indeed, spontaneous departure from the lysogenic state is rare, occurring at a frequency of less than once per million cell-generations (Aurell *et al.* 2002, Bæk *et al.* 2003).

Anthenelli *et al.* (2020) suggested that a virus incorporating into the bacterial host genome can be viewed as a "rachet" that they describe a process involving a reorganization of virus/bacteria community structure during microbialization. The prophage lock here is a wholly different idea that relies on the fitness advantage to a prophage of remaining in its host genome provided it carries a gene benefiting the host. Also, Sudhakari and Ramisetty (2023) have described the "grounding" of prophages in the host genome. They note that most putative prophages are relics of past phage/bacteria conflicts and consider them as "grounded" because they can no longer be excised from the bacterial genome. They interpret the grounding a result of phage/bacteria conflicts whereby the bacteria "win" by grounding the prophage in their genome to confer immunity to superinfection.

Virus as Vectors of Horizontal Gene Transfer

Virus can bring about horizontal gene transfer (HGT) (Canchaya *et al.* 2003, Gilbert and Cordaux 2017, Borodovich *et al.* 2022, Irwin *et al.* 2022). Prophage in one bacterial line can "pick up" a fragment of the host DNA that contains a gene, transition to the lytic phase, then infect other bacterial lines and ultimately transition back to a prophage in another bacterial line whereupon the foreign DNA is expressed there. The evolutionary question is why a virus should conveniently serve as a vehicle for transporting genes from one bacterial lineage to another.

The switch function, Eq. 17, suggests a scenario in which horizontal gene transfer makes evolutionary sense for the virus regardless of its effect on the bacteria. Suppose the bacterial environment is in continual fluctuation. If so, a high R supporting a lysogenic life cycle may fluctuate down to a low R favoring a lytic life cycle, whereupon the virus releases from the bacterial genome and lyses into the environment as virions. Next, these particles infect other bacteria. If R should fluctuate back up to a high value favoring a lysogenic life cycle, then the newly infecting virus incorporate into the genome of their new hosts and express their gene-containing fragment there.

This scenario derived from the model's switch function predicts that horizontal gene transfer should proceed at a higher rate in fluctuating environments than in quiescent environments.

Three-Level (Tripartite) Holobionts

Holobionts consisting of three levels—virus, bacteria and eukaryotic host, often called "tripartite" holobionts, are receiving increased attention (Moran *et al.* 2005, Bordenstein *et al.* 2006, Kelly *et al.* 2014, Keen and Dantas 2018, Barr 2019, Belleghem *et al.* 2019, Bodner *et al.* 2021, Wahida *et al.* 2021, Zheng *et al.* 2023). A question raised by these contributions is whether a prophage gene expressed in a bacterium that itself resides in the microbiome of a eukaryotic host can improve the fitness of the eukaryotic host, producing a tripartite hologenome.

For viral-carried gene to affect the fitness of the host in a holobiont, a temperate virus must first be incorporated as a prophage into the bacterium—Eq. 17, Case B supplies the condition for this to occur. Next, the prophage-containing bacterium must be incorporated into the host's microbiome. The process for entry into the host's microbiome is host-orchestrated species sorting (HOSS, Roughgarden 2023). By this process, the bacteria must offer enough benefit to the host to avoid its exclusion by the host immune response. If a gene in the prophage of a bacterium in the host's microbiome causes the bacterium to allocate sufficient resources to the host, then the host relaxes its immune screening of the bacterium and the prophage-containing bacterium becomes integrated in the host's hologenome forming a three-level symbiosis. Thus, a gene in the prophage of a bacterium can theoretically contribute to holobiont fitness as a component of the hologenome provided the gene causes the bacterium it inhabits to contribute enough to the host fitness that it is allowed into the host's microbiome—the result is a functionally integrated tripartite holobiont.

Discussion

This paper introduces a simple model for the population dynamics of virulent phage and bacteria that features infection of bacteria by Poisson sampling of viral particles from the environment rather than mass-action collisions of virus with bacteria. Also, the new model is developed in discrete time with a time step equal to the viral latency period, rather than in continuous time and does not require assuming density-dependent bacterial population growth. The source of density dependence in the model lies in the kinetics of viral absorption onto the bacterial surface.

The model of virulent-phage bacteria population dynamics was extended to temperate phage. The condition for transition from a lytic to lysogenic phase was derived as a formula termed the "fitness switch". The virus switches from lytic to lysogenic when its population grows faster with prophage than as virions produced by lysis of the infected cell. The switch function compares the product, (base absorption probability $\times$ the per-virus burst size), with the bacterial population geometric growth factor, R.

The switch function is used to predict temperate viral-bacteria dynamics in several environmental scenarios: intervention that lowers probability of absorption, environmental deteriora-

tion that affects both virus and bacteria, the ecogeographic rule that environmental enrichment increases bacterial population growth (microbialization), fluctuating environmental conditions that promote horizontal gene transfer (HGT), and the integration of a prophage-containing bacteria population into the microbiome of a eukaryotic host that leads to a functionally integrated tripartite holobiont.

The purpose of the model is to understand qualitatively what is happening during the phage/bacteria interaction. It is not to predict the exact course of phage/bacteria population dynamics. That would presumably require constructing a chemostat-like experimental setup and accurately measuring both the model parameters and the virus and bacterial abundance during the course of the experiment—an expense not clearly worth its scientific insight.

Instead, the key features of the model worth explicit testing are the condition for increase when rare, Eq. 11, that is the criterion for when a lytic phage and bacteria can coexist and the extension of this criterion as the fitness switch, Eq. 17, that is the basis for the model's many qualitative predictions. The increase-when-rare condition would be tested with a lytic virus in an experimental setup wherein the virus a_o and b_o parameters were measured along with the bacterial R. If the R were experimentally raised by augmenting bacterial resources from a low value at which $a_o\, b_o > R$ to a higher value at which $a_o\, b_o < R$, then the lytic virus should infect at low R and fail to infect at high R. The threshold R between success and failure to infect should occur when R satisfies $a_o\, b_o = R$.

The fitness switch condition would be similarly tested with a temperate virus. If the R were experimentally raised from a low value, the prediction is that the virus would integrate when passing the threshold at which $a_o\, b_o = R$. That is, initially when $a_o\, b_o > R$, virus added to a bacteria population should infect and then lyse and when $a_o\, b_o < R$ the introduced virus should infect and then integrate. The integration is presumably measured by noting that the concentration of viral integrase enzymes suddenly rises from a low level to a high level as the threshold is passed. Undoubtedly experimentalists can suggest better setups than the author.

Another feature needing explicit test is the model's assumption of density-dependent absorption. Studies of viral absorption kinetics like those cited earlier in the paper should be conducted in the future at a full range of multiplicities of infection (MOI).

The model can be extended to account for additional phenomena. Notable among these is the evolution of phage resistance by the bacteria. The rise of antibiotic drug resistance in bacteria is fueling interest in phage therapy as a possible way to kill these pathogenic bacteria. But the prospects for using phages as biological control are tempered by the ability of the bacteria to evolve resistance to infection by phages (Azam and Tanji 2019, Monteiro *et al.* 2019, Torres-Barceló *et al.* 2022). Also, virus have been discovered to communicate with one another (Harms and Diard 2019, Rajaure and Adhya 2019, Brady *et al.* 2021, Bruce *et al.* 2021). A future paper building on this paper's model will explore theoretically the coevolution of phage with bacteria

and specifically, the evolution of phage resistance.

This paper's model is relevant to hypotheses in the virus ecology literature about how viruses influence microbial community structure. Thingstad (Thingstad and Lignell 1997, Thingstad 2000, Winter *et al.* 2020) advanced a hypothesis known as "Kill the Winner" (KtW). The idea is that a bacteria population that happens to be abundant is, as a result of its abundance, subject to more infection from lytic viruses than less abundant bacteria. Thingstad refers to this effect as "negative frequency selection" and explicitly cites the Lotka-Volterra predator-prey equations as the starting point for a KtW model. That is, when the prey abundance increases, the predator abundance increases soon thereafter, chopping down a temporary excess of prey. When extended to multiple species of bacteria, the hypothesis is that whenever one bacterial strain increases, perhaps because of being a better competitor, its success is countered by increased viral infection, thereby preventing any one bacterial strain from dominating. This process is hypothesized to maintain microbial diversity. Lytic virus are thus envisioned as keystone predators.

Lytic viruses that control an algal bloom in the way envisioned under KtW were documented by Bratbak *et al.* (1993) who report that blooms of a marine coccolithophorid off the coast of Norway were in some cases succeeded by an increase in the abundance of viruses. They further report that viral lysis could account for 25 to 100% of the net mortality of the coccolithophorids and that by the time the blooms declined the concentration of free algal viruses was seen to have increased. However, Evans and Brussaard (2012) report that in the Southern Ocean both viral lysis and microzooplankton grazing together control cyanobacterial populations, whereas viral control of eukaryotic algae was comparatively minor. And finally, Needham *et al.* (2013) report that off the coast of California near Santa Catalina Island common bacterial and viral taxa were consistently dominant and that "relatively few displayed dramatic increases/decreases or 'boom/bust' patterns that might be expected from dynamic predator-prey interactions." Thus, empirical support for the picture envisioned in the KtW hypothesis is mixed.

The model in this paper is not consistent with a KtW picture based on the Lotka-Volterra predator-prey model because in this paper's model, a lytic virus population comes to equilibrium with its bacterial host. In this paper's model, the virus and bacteria do not oscillate as they do in a Lotka-Volterra-like model such as Campbell (1961). Hence, in this paper's model the virus population does not chase abundant bacteria chopping down their abundance and killing the winner. Instead, in this paper's model, the lytic virus coexists with the winner even though this may result in the exclusion of the losers and an accompanying loss of microbial diversity.

Furthermore, according to the KtW picture, a high abundance of winning bacterial strains should soon be followed by a high abundance of virus that are in the process of killing the winners, resulting in a high virus to microbe ratio (VMR) in the environment. However, Forest Rohwer and colleagues (Knowles *et al.* 2016) demonstrated across multiple ecosystems and laboratory situations that virus are relatively less abundant in the environment when occurring with

high bacterial densities. Specifically, microbialization on coral reefs along with their elevated bacterial abundances is associated with low VMR rather than high VMR as expected by the KtW hypothesis.

As a result, Rohwer and colleagues (Knowles *et al.* 2016, Silveira and Rohwer 2016) proposed an alternative hypothesis they termed "Piggyback the Winner" (PtW). By this hypothesis, virus become lysogenic in conditions of high bacterial abundance resulting in few virus particles being found outside the bacterial cells because they are residing inside the bacteria as prophages, leading to a low VMR.

On its face, the fitness switch in this paper supports the PtW hypothesis because, as mentioned earlier, the higher R in the nutrient-rich eutrophic conditions that cause microbialization leads to satisfying Condition B in Eq. 17, indicating a switch from lysis to lysogeny.

In contrast to the fitness-switch theory espoused in this paper, Silveira and Rohwer (2016) propose a hypothesis for the increase in lysogeny during microbialization based on the observation that mucosal surfaces in microbialized environments facilitate viral colonization of bacteria (Barr *et al.* 2015). However, this increases the absorption parameter, a_o in Eq. 17, favoring the lytic phase according to Condition A rather than the lysogenic phase according to Condition B. So, according to the fitness switch model, an increased rate of phage-bacteria encounters in mucus cannot explain the increase in lysogeny during microbialization because the argument goes the wrong way.

Alternatively, Luque and Silveira (2020) also note that the high viral densities in microbialized situations leads to increased coinfections which is known to promote lysogeny, as discussed earlier. This might contribute to favoring lysogeny. However, increasing DOM increases the bacterial R and can flip the fitness switch from lytic to lysogeny by itself. Therefore, this paper is consistent with the PtW hypothesis if understood as follows: the reason for PtW is the high R associated with eutrophication, although a role for increased coinfection in eutrophic conditions cannot be ruled out.

KtW and PtW need not necessarily be viewed as competing hypotheses. Indeed, Chen *et al.* (2021) argue that KtW and PtW "are not mutually exclusive and need to be combined." Alternatively, one might simply stipulate that KtW pertains only to lytic viruses whereas PtW pertains only to temperate viruses. With this stipulation, whether KtW is correct for lytic virus can be examined on its own merits regardless of whether PtW is also correct for temperate virus, and *vice versa*.

Acknowledgments

The author thanks Forest Rohwer, Toni Luque, Sergio Cobo-Lopez, James Nulton and Anca Segall of the SDSU BioMath Group, Seth Bordenstein, Sarah Bordenstein, Andrew Read, Ottar

Bjørnstad and members of the Penn State Microbiome Center, and Jaime G. Lopez of the Stanford Medical School for discussion about this paper. The author also thanks two anonymous reviewers for helpful comments. This article is Contribution #2 from a project, The Theory of Holobiont Evolution, funded by the Gordon and Betty Moore Foundation through Grant GBMF10000 to the University of Hawaii.

References

This section includes references cited in the Supplementary Material.

Anderson, R. M. and May, R. M. 1979. "Population Biology of Infectious Diseases: Part I." Nature 280, 361–367.

Anthenelli, Maxwell, Emily Jasien, Robert Edwards, Barbara Bailey, Ben Felts, Parag Katira, James Nulton, Peter Salamon, Forest Rohwer, Cynthia B. Silveira, Antoni Luque 2020 Phage and bacteria diversification through a prophage acquisition ratchet. bioRxiv 2020.04.08.028340; doi: https://doi.org/10.1101/2020.04.08.028340

Aurell, E., Brown, S., Johanson, J. & Sneppen, K. 2002. Stability puzzles in phage. Phys. Rev. ser. E, 65, 05191.

Azam, A.H., Tanji, Y. 2019. Bacteriophage-host arm race: an update on the mechanism of phage resistance in bacteria and revenge of the phage with the perspective for phage therapy. Appl Microbiol Biotechnol 103, 2121–2131. https://doi.org/10.1007/s00253-019-09629-x

Baiser, B., Dominique Gravel, Alyssa R. Cirtwill, Jennifer A. Dunne, Ashkaan K. Fahimipour, Luis J. Gilarranz, Joshua A. Grochow, Daijiang Li, Neo D. Martinez, Alicia McGrew, Timothée Poisot, Tamara N. Romanuk, Daniel B. Stouffer, Lauren B. Trotta, Fernanda S. Valdovinos, Richard J. Williams, Spencer A. Wood, Justin D. Yeakel. 2019. Ecogeographical rules and the macroecology of food webs. Global Ecol Biogeogr. 2019; 28: 1204–1218. https://doi.org/10.1111/geb.12925

Bæk, K. T., Svenningsen, S. L., Eisen, H., Sneppen, K., & Brown, S. (2003). Single-cell Analysis of Lambda Immunity Regulation. Journal of Molecular Biology, 334(3), 363–372. https://doi.org/10.1016/j.jmb.2003.09.037

Barr, Jeremy J., Rita Auro, Nicholas Sam-Soon, Sam Kassegne, Gregory Peters, Natasha Bonilla, Mark Hatay,Sarah Mourtad, Barbara Bailey, Merry Youle, Ben Felts, Arlette Baljon, Jim Nulton, Peter Salamon,and Forest Rohwer 2015 Subdiffusive motion of bacteriophage in mucosal surfaces increases the frequency of bacterial encounters. Proc. Natl Acad. Sci. USA 112, 13675–13680

Barr J. J. 2019. Missing a Phage: Unraveling Tripartite Symbioses within the Human Gut. mSystems, 4(3), e00105-19. https://doi.org/10.1128/mSystems.00105-19

Bednarz, Michael, Jennifer A. Halliday, Christophe Herman, Ido Golding 2014. Revisiting Bistability in the Lysis/Lysogeny Circuit of Bacteriophage Lambda. PLOS ONE www.plosone.org 9(6):e100876

Beretta, E. and Y. Kuang 1998. Modeling and analysis of a marine bacteriophage infection. Mathematical Biosciences 149 57–76

Beretta E. and Y. Kuang. 2001. Modeling and analysis of a marine bacteriophage infection with latency period. Nonlinear Anal Real World Appl 2:35–74.

Bjørnstad, Ottar 2018. Epidemics: Models and Data using R. Springer Nature Switzerland AG. https://doi.org/10.1007/978-3-319-97487-3, Second Edition, 2023.

Bobay, Louis-Marie, Marie Touchon and Eduardo P C Rocha. 2014. Pervasive domestication of defective prophages by bacteria. Proc. Nat Acad Sci (USA) 111:12127–12132, www.onas.ora/cal/d0l/10.1073/onas.1405336111

Bodner, Katie, Arin L. Melkonian, Markus W. Covert, 2021 The Enemy of My Enemy: New Insights Regarding Bacteriophage–Mammalian Cell Interactions, Trends in Microbiology, Volume 29, Issue 6, 2021, Pages 528–541, ISSN 0966-842X, https://doi.org/10.1016/j.tim.2020.10.014.

Bondy-Denomy, Joseph and Alan R. Davidson 2014. When a Virus is not a Parasite: The Beneficial Effects of Prophages on Bacterial Fitness. Journal of Microbiology (2014) Vol. 52, No. 3, pp. 235–242. DOI 10.1007/s12275-014-4083-3

Bordenstein SR, Marshall ML, Fry AJ, Kim U, Wernegreen JJ 2006 The tripartite associations between bacteriophage, Wolbachia, and arthropods. PLoS Pathog 2(5): e43. DOI: 10.1371/journal.ppat.0020043

Borodovich, T., Shkoporov, A. N., Ross, R. P., & Hill, C. 2022. Phage-mediated horizontal gene transfer and its implications for the human gut microbiome. Gastroenterology report, 10, goac012. https://doi.org/10.1093/gastro/goac012

Brady, Aisling, Nuria Quiles-Puchalt, Francisca Gallego del Sol, Sara Zamora-Caballero, Alonso Felipe-Ruíz, Jorge Val-Calvo, Wilfried J.J. Meijer, Alberto Marina, and José R. Penadés 2021. The arbitrium system controls prophage induction. Current Biology 31:5037–5045 https://doi.org/10.1016/j.cub.2021.08.072

Bratbak, Gunnar, Jorun K. Egge, and Mikal Heldal. 1993 "Viral Mortality of the Marine Alga Emiliania Huxleyi (Haptophyceae) and Termination of Algal Blooms." Marine Ecology Progress Series 93, no. 1/2 (1993): 39–48. http://www.jstor.org/stable/24832806.

Breitbart M, Bonnain C, Malki K, Sawaya N 2018. Phage puppet masters of the marine microbial realm. Nat Microbiol 3:754–66.

Brown, Christopher M. and Kay D. Bidle. 2014. Attenuation of virus production at high multiplicities of infection in *Aureococcus anophagefferens*. Virology 466-467 (2014) 71–81. http://dx.doi.org/10.1016/j.virol.2014.07.023

Bruce, John B., Sebastien Lion, Angus Buckling, Edze R. Westra, and Sylvain Gandon 2021. Regulation of prophage induction and lysogenization by phage communication systems. Current Biology 31:5046–5051 https://doi.org/10.1016/j.cub.2021.08.073

Bull, J. J., J. Millstein, J. Orcutt and H. A. Wichman 2006. Evolutionary Feedback Mediated through Population Density, Illustrated with Viruses in Chemostats. The American Naturalist , Vol. 167, No. 2 pp. E39–E51 https://www.jstor.org/stable/10.1086/499374

Campbell, Allan. 1961. Conditions for the Existence of Bacteriophage. *Evolution* 15:153–165.

Campbell, Allan. 1981 Evolutionary Significance of Accessory DNA Elements in Bacteria, Ann. Rev. Microbiol. 35:55–83

Canchaya, C., Fournous, G., Chibani-Chennoufi, S., Dillmann, M. L., & Brüssow, H. 2003. Phage as agents of lateral gene transfer. Current opinion in microbiology, 6(4), 417–424. https://doi.org/10.1016/s1369-5274(03)00086-9

Chen, Xiaowei ; Markus G. Weinbauer, Nianzhi Jiao, Rui Zhang 2021. Revisiting marine lytic and lysogenic virus-host interactions: Kill-the-Winner and Piggyback-the-Winner. Science Bulletin 66 (2021) 871–874

Cheong, Kang Hao; Tao Wena, Sean Benler, Jin Ming Koh, and Eugene V. Koonin 2022. Alternating lysis and lysogeny is a winning strategy in bacteriophages due to Parrondo's paradox. PNAS 2022 Vol. 119 No. 13 e2115145119 https://doi.org/10.1073/pnas.2115145119

Davies, Emily V., Craig Winstanley, Joanne L. Fothergill and Chloe E. James 2016. The role of temperate bacteriophages in bacterial infection. FEMS Microbiology Letters, 363, 2016, fnw015. doi: 10.1093/femsle/fnw015

Diekmann, Odo, Hans Heesterbeek and Tom Britton 2013. Mathematical Tools for Understanding Infectious Disease Dynamics. Princeton University Press. Volume 7 in the series Princeton Series in Theoretical and Computational Biology
https://doi.org/10.1515/9781400845620

Dimitrov, D. 2004. Virus entry: molecular mechanisms and biomedical applications. Nat Rev Microbiol 2, 109–122 2004. https://doi.org/10.1038/nrmicro817

Ding, Hui and Liao-Fu Luo 2009. Kinetic Model of the Lysogeny/Lysis Switch of Phage λ. Chin. Phys. Lett. Vol.26,No.9(2009)098701

Echeverría-Vega, A., Morales-Vicencio, P., Saez-Saavedra, C., Alvarez, M. A., Gordillo, F., Del-Valle, R., Solís, M. E., and Araya, R. (2020). Characterization of the Bacteriophage vB_VorS-PVo5 Infection on Vibrio ordalii: A Model for phage/bacteria Adsorption in Aquatic Environments. Frontiers in microbiology, 11, 550979. https://doi.org/10.3389/fmicb.2020.550979

Ellis, E., and M. Delbrück. 1939. "The Growth of Bacteriophage." *J. General Physiology* 22:365–384. doi: 10.1085/jgp.22.3.365

Endy D, Kong D, Yin J. 1997 Intracellular kinetics of a growing virus: a genetically structured simulation for bacteriophage T7. Biotechnol Bioeng. Jul 20 55(2):375–89.

Evans, Claire and Corina P. D. Brussaard 2012 Viral lysis and microzooplankton grazing of phytoplankton throughout the Southern Ocean. Limnol. Oceanogr., 57(6), 2012, 1826–1837

Foster-Nyarko, Ebenezer and Mark J. Pallen 2022 The microbial ecology of *Escherichia coli* in the vertebrate gut. FEMS Microbiology Reviews, 46, 1–22 DOI: 10.1093/femsre/fuac008

Fry, B. A.,1959. Conditions for the Infection of Escherichia coli with Lambda Phage and for the Establishment of Lysogeny. J .gen.Microbiol. 21:676–684.

Gadagkar, Raghavendra and K. P. Gopinathan 1980 Bacteriophage burst size during multiple infections. J. Biosci., Vol. 2, Number 3, September 1980, pp. 253–259.

Gaston, K.J., Chown, S.L. and Evans, K.L. 2008, Ecogeographical rules: elements of a synthesis. Journal of Biogeography, 35: 483-500. https://doi.org/10.1111/j.1365-2699.2007.01772.x

Gibson B, Wilson DJ, Feil E, Eyre-Walker A. 2018 The distribution of bacterial doubling times in the wild. Proc. R. Soc. B 285: 20180789. http://dx.doi.org/10.1098/rspb.2018.0789

Gilbert, C., & Cordaux, R. (2017). Viruses as vectors of horizontal transfer of genetic material in eukaryotes. Current opinion in virology, 25, 16–22. https://doi.org/10.1016/j.coviro.2017.06.005

Giljan, G., Kamennaya, N.A., Otto, A., Becher, D., Ellrott, A., Meyer, V., Bramley J. Murton, Bernhard M. Fuchs, Rudolf I. Amann & Mikhail V. Zubkov (2020) Bacterioplankton reveal years-long retention of Atlantic deep-ocean water by the tropic sea-mount. Sci Rep 10: 1–11.

Grove, Joe , Mark Marsh; 2011 The cell biology of receptor-mediated virus entry. J Cell Biol 26 December 2011; 195 (7): 1071–1082. doi: https://doi.org/10.1083/jcb.201108131

Haas, A., Fairoz, M., Kelly, L. *et al.* 2016. Global microbialization of coral reefs. Nature Microbiol 1, 16042. https://doi.org/10.1038/nmicrobiol.2016.42

Harms, Alexander and Médéric Diard 2019 Crowd Controlled—Host Quorum Sensing Drives Phage Decision. Cell Host & Microbe 25:179–181. https://doi.org/10.1016/j.chom.2019.01.016

Harvell CD, Kim K, Burkholder JM, Colwell RR, Epstein PR, Grimes DJ, Hofmann EE, Lipp EK, Osterhaus AD, Overstreet RM, Porter JW, Smith GW, Vasta GR. Emerging marine diseases—climate links and anthropogenic factors. Science. 1999 Sep 3;285(5433):1505-10. doi: 10.1126/science.285.5433.1505. PMID: 10498537.

Huang, Gang, Yasuhiro Takeuchi, and Wanbiao MA. 2010. Lyapunov Functionals for Delay Differential Equations. Model of Viral Infections. Siam J. Appl. Math Vol. 70, No. 7, pp. 2693–2708

Hubbs NB, Whisby-Pitts MM, McMurry JL. 2019 Kinetic analysis of bacteriophage Sf6 binding to outer membrane protein a using whole virions. Acta Virol. 63(4):450-458. doi: 10.4149/av_2019_412. PMID: 31802688.

Huss, Phil, Anthony Meger, Megan Leander, Kyle Nishikawa and Srivatsan Raman (2021) Mapping the functional landscape of the receptor binding domain of T7 bacteriophage by deep mutational scanning eLife 10:e63775 https://doi.org/10.7554/eLife.63775

Irwin, N.A.T., Pittis, A.A., Richards, T.A. et al. Systematic evaluation of horizontal gene transfer between eukaryotes and viruses. Nat Microbiol 7, 327–336 (2022). https://doi.org/10.1038/s41564-021-01026-3

Jarett, J. K., Mária Džunková, Frederik Schulz, Simon Roux, David Paez-Espino, Emiley Eloe-Fadrosh, Sean P. Jungbluth, Natalia Ivanova, John R. Spear, Stephanie A. Carr, Christopher B. Trivedi, Frank A. Corsetti, Hope A. Johnson, Eric Becraft, Nikos Kyrpides, Ramunas Stepanauskas, and Tanja Woyke. 2020 Insights into the dynamics between viruses and their hosts in a hot spring microbial mat. ISME J. 14, 2527–2541 (2020).

Keeling, M. J., & Rohani, P. (2008). Modeling infectious diseases in humans and animals. Princeton, NJ: Princeton University Press.

Keen, Eric C., Gautam Dantas, 2018 Close Encounters of Three Kinds: Bacteriophages, Commensal Bacteria, and Host Immunity, Trends in Microbiology, 26:943–954

Kermack, W. O. and McKendrick, A. G. 1927 "A Contribution to the Mathematical Theory of Epidemics." Proc. Roy. Soc. Lond. A 115, 700–721.

Kelly, Linda W., Gareth J. Williams, Katie L. Barott, Craig A. Carlson, Elizabeth A. Dinsdale, Robert A. Edwards, Andreas F. Haas, Matthew Haynes, Yan Wei Lima, Tracey McDole, Craig E. Nelson, Enric Sala, Stuart A. Sandin, Jennifer E. Smith, Mark J. A. Vermeij, Merry Youle, and Forest Rohwer. 2014. Local genomic adaptation of coral reef-associated microbiomes to gradients of natural variability and anthropogenic stressors. Proc. Nat. Acad. Sci. (USA) 111(28) 10227–10232. www.pnas.org/cgi/doi/10.1073/pnas.1403319111

Kim, Min-Soo and Jin-Woo Bae. 2018. Lysogeny is prevalent and widely distributed in the murine gut microbiota. The ISME Journal 12:1127–1141 https://doi.org/10.1038/s41396-018-0061-9

Koehler, Melanie, Martin Delguste, Christian Sieben, Laurent Gillet and David Alsteens 2020. Initial Step of Virus Entry: Virion Binding to Cell-Surface Glycans. Annual Review of Virology 7:143–65 https://doi.org/10.1146/annurev-virology-122019-070025

Knowles, B., C. B. Silveira, B. A. Bailey, K. Barott, V. A. Cantu, A. G. Cobián-Güemes, F. H. Coutinho, E. A. Dinsdale, B. Felts, K. A. Furby, E. E. George, K. T. Green, G. B. Gregoracci, A. F. Haas, J. M. Haggerty, E. R. Hester, N. Hisakawa, L. W. Kelly, Y. W. Lim, M. Little, A. Luque, T. McDole-Somera, K. McNair, L. S. de Oliveira, S. D. Quistad, N. L. Robinett, E. Sala, P. Salamon, S. E. Sanchez, S. Sandin, G. G. Z. Silva, J. Smith, C. Sullivan, C. Thompson, M. J. A. Vermeij, M. Youle, C. Young, B. Zgliczynski, R. Brainard, R. A. Edwards, J. Nulton, F. Thompson & F. Rohwer 2016. Lytic to temperate switching of viral communities. Nature 531: 466–470

Koonjan S, Cardoso Palacios C, Nilsson AS. Population Dynamics of a Two Phages–One Host Infection System Using Escherichia coli Strain ECOR57 and Phages vB_EcoP_SU10 and vB_EcoD_SU57. Pharmaceuticals. 2022; 15(3):268. https://doi.org/10.3390/ph15030268

Kourilsky P. 1973. Lysogenization by bacteriophage lambda. I. Multiple infection and the lysogenic response. Mol. Gen. Genet. 122:183–95

Kourilsky P, Knapp A. 1974. Lysogenization by bacteriophage lambda. III. Multiplicity dependent phenomena occurring upon infection by lambda. Biochimie 56:1517–23

Krysiak-Baltyn, Konrad , Gregory J. O. Martin, Anthony D. Stickland, Peter J. Scales, and Sally L. Gras 2016. Computational models of populations of bacteria and lytic phage. Crit Rev Microbiol, 2016; 42(6): 942–968 DOI: 10.3109/1040841X.2015.1114466

Levin, Bruce R. , Frank M. Stewart, and Lin Chao 1977 Resource-limited growth, Competition, and Predation: A model and Experimental Studies with Bacteria and Bacteriophage. Amer. Natur. 111:3–24.

Lomolino, M.V., Sax, D.F., Riddle, B.R. and Brown, J.H. 2006, The island rule and a research agenda for studying ecogeographical patterns. Journal of Biogeography, 33: 1503-1510. https://doi.org/10.1111/j.1365-2699.2006.01593.x

Luque A, Silveira CB. 2020. Quantification of lysogeny caused by phage coinfections in microbial communities from biophysical principles. mSystems 5:e00353-20. https://doi.org/10.1128/mSystems.00353-20

Yi, Y., Liu, S., Hao, Y., Qingyang Sun, Xinjuan Lei, Yecheng Wang, Jiahua Wang, Mujie Zhang, Shan Tang, Qingxue Tang, Yue Zhang, Xipeng Liu, Yinzhao Wang, Xiang Xiao & Huahua Jian. 2023 A systematic analysis of marine lysogens and proviruses. Nat Commun 14, 6013 https://doi.org/10.1038/s41467-023-41699-4

López-Leal, Gamaliel, Laura Carolina Camelo-Valera, Juan Manuel Hurtado-Ramírez, Jérôme Verleyen, Santiago Castillo-Ramírez, Alejandro Reyes-Muñoza 2022. Mining of Thousands of Prokaryotic Genomes Reveals High Abundance of Prophages with a Strictly Narrow Host Range. mSystems 7:4 10.1128/msystems.00326-22.

Luo, E., Eppley, J.M., Romano, A.E., Mende, D.R., and DeLong, E.F. (2020) Double-stranded DNA virioplankton dynamics and reproductive strategies in the oligotrophic open ocean water column. ISME J 14: 1304–1315.

Mackey, Michael C., Moisés Santillán, Marta Tyran-Kamińska, Eduardo S. Zeron 2016. Simple Mathematical Models of Gene Regulatory Dynamics. Lecture Notes on Mathematical Modelling in the Life Sciences. Springer International Publishing Switzerland

Maginnis, Melissa S. 2018. Virus–Receptor Interactions: The Key to Cellular Invasion. J Mol Biol (2018) 430, 2590–2611 https://doi.org/10.1016/j.jmb.2018.06.024

May, Robert. 1976. Simple mathematical models with very complicated dynamics. Nature 261:459–467.

Mizuno, C. M., Ghai, R., Saghaï, A., López-García, P. & Rodriguez-Valera, F. 2016 Genomes of abundant and widespread viruses from the deep ocean. mBio 7, e00805–e00816.

Moldovan, R., Chapman-McQuiston, E., and Wu, X. L. (2007). On kinetics of phage adsorption. Biophysical journal, 93(1), 303–315. https://doi.org/10.1529/biophysj.106.102962

Monteiro, Rodrigo, Diana Priscila Pires, Ana Rita Costa, and Joana Azeredo 2019. Phage Therapy: Going Temperate? Trends in Microbiology, 27:4 https://doi.org/10.1016/j.tim.2018.10.008

Moran, Nancy & Degnan, Patrick & Santos, Scott & Dunbar, Helen & Ochman, Howard. (2005). The players in a mutualistic symbiosis: Insects, bacteria, viruses, and virulence genes. Proceedings of the National Academy of Sciences of the United States of America. 102. 16919–26. 10.1073/pnas.0507029102.

Needham, David M ; Cheryl-Emiliane T Chow, Jacob A Cram, Rohan Sachdeva, Alma Parada and Jed A Fuhrman 2013. Short-term observations of marine bacterial and viral communities: patterns, connections and resilience. The ISME Journal (2013) 7, 1274–1285.

Nicholson, A. J. and V. A. Bailey 1935. The Balance of Animal Populations.—Part I. Proceedings of the Zoological Society of London. 105:551–598 https://doi.org/10.1111/j.1096-3642.1935.tb01680.x

Obeng, Akbar, Adjie Pratama, and Jan Dirk van Elsas 2016. The Significance of Mutualistic Phages for Bacterial Ecology and Evolution. Trends in Microbiology, June 2016, Vol. 24, No. 6 http://dx.doi.org/10.1016/j.tim.2015.12.009

O'Malley, M. 2016. The ecological virus. Studies in History and Philosophy of Biological and Biomedical Sciences 59 (2016) 71–79. http://dx.doi.org/10.1016/j.shpsc.2016.02.012

Parada, Verònica , Gerhard J. Herndl and Markus G. Weinbauer. 2006. Viral burst size of heterotrophic prokaryotes in aquatic systems. J. Mar. Biol. Ass. U.K. 86, 613–621

Patel, I. R. and K. K. Rao. 1984. Bacteriophage burst size as a function of multiplicity of infection. Current Science 53:198–200.

Philipson L. (1983). Attachment of viruses to cell receptors and penetration of viruses into cells. Textbook of Medical Virology, 51–56. https://doi.org/10.1016/B978-0-407-00253-1.50012-8

Prashant K. Purohit, Mandar M. Inamdar, Paul D. Grayson, Todd M. Squires, Janè Kondev, and Rob Phillips 2005 Forces during bacteriophage DNA packaging and ejection. Biophys J. Feb88(2):851–66. (p.852 caption to figure 1)

Prasith Baccam, Catherine Beauchemin, Catherine A. Macken, Frederick G. Hayden, and Alan S. Perelson 2006 Kinetics of Influenza A Virus Infection in Humans. Journal of Virlogy, Aug. 2006, p. 7590–7599 Vol. 80, No. 15 doi:10.1128/JVI.01623-05

Rajaure, Manoj and Sankar Adhya 2019. Molecular Basis of Phage Communication. Molecular Cell 74:1–2. https://doi.org/10.1016/j.molcel.2019.03.015

Ranasinghe, Nilakshi 2019. Literature study of virus size, burst size, latent period and genome size across different lytic eukaryotic and prokaryotic virus groups—an overview of traits and possible trade-offs. MSc Thesis. Department of biology, University of Bergen

Roughgarden, J. 1996. Appendix A3: Matrix Algebra and Stability Theory. Pp. 556–581 in: Roughgarden. 1996. Theory of Population Genetics and Evolutionary Ecology, An Introduction. Prentice Hall, Upper Saddle River, NJ.

Roughgarden, J. 1998. *Primer of Ecological Theory*. Prentice Hall. New Jersey.

Roughgarden, J., S. F. Gilbert, E. Rosenberg, I. Zilber-Rosenberg, and E. Lloyd. 2018. Holobionts as units of selection and a model of their population dynamics and evolution. Biological Theory 13:44–65, https://doi.org/10.1007/s13752-017-0287-1.

Roughgarden, J. 2020. Holobiont evolution: mathematical model with vertical vs. horizontal microbiome transmission. Philosophy, Theory and Practice in Biology, 12:2. http://dx.doi.org/10.3998/ptpbio.16039257.0012.002.

Roughgarden, J. 2023. Holobiont Evolution: Population Theory for the Hologenome. The American Naturalist, https://doi.org/10.1086/723782.

Santillán, Moisés and Michael C. Mackey 2004. Why the Lysogenic State of Phage λ Is So Stable: A Mathematical Modeling Approach Biophysical Journal Volume 86 January 2004 75–84

Schaffer, William M. 1983. The Application of Optimal Control Theory to the General Life History Problem. The American Naturalist, 121:418–431.

Shivam, Shashwat, Guanlin Li, Adriana Lucia-Sanz and Joshua S. Weitz 2022. Timescales modulate optimal lysis–lysogeny decision switches and near-term phage reproduction. Virus Evolution 8:1–18 DOI: https://doi.org/10.1093/ve/veac037

Silveira Cynthia B and Forest L Rohwer 2016 Piggyback-the-Winner in host-associated microbial communities. npj Biofilms and Microbiomes 2, 16010; doi:10.1038/npjbiofilms.2016.10

Silveira, Cynthia B., Felipe H. Coutinho, Giselle S. Cavalcanti, Sean Benler, Michael P. Doane, Elizabeth A. Dinsdale, Robert A. Edwards, Ronaldo B. Francini-Filho, Cristiane C. Thompson, Antoni Luque, Forest L. Rohwer and Fabiano Thompson. 2020. Genomic and ecological attributes of marine bacteriophages encoding bacterial virulence genes. BMC Genomics 21:126 https://doi.org/10.1186/s12864-020-6523-2

Silveira, Cynthia B., Antoni Luque and Forest Rohwer 2021. The landscape of lysogeny across microbial community density, diversity and energetics. Environmental Microbiology 23:4098–4111

Sinha V, Goyal A, Svenningsen SL, Semsey S and Krishna S (2017) In silico Evolution of Lysis-Lysogeny Strategies Reproduces Observed Lysogeny Propensities in Temperate Bacteriophages. Front. Microbiol. 8:1386. doi: 10.3389/fmicb.2017.01386

Sudhakari, Pavithra Anantharaman and Bhaskar Chandra Mohan Ramisetty 2023. An Eco-evolutionary Model on Surviving Lysogeny Through Grounding and Accumulation of Prophages. Microbial Ecology https://doi.org/10.1007/s00248-023-02301-y

Stewart, Frank M., and Bruce R. Levin 1984. The Population Biology of Bacterial Viruses: Why Be Temperate. Theoretical Population Biology. 26, 93–117

Suttle CA. 2007. Marine viruses—major players in the global ecosystem. Nat Rev Microbiol 5:801–12.

Tang, X. H. and Xingfu Zou. 2008. Global Attractivity in a Predator-Prey System with Pure Delays. Proceedings of the Edinburgh Mathematical Society (2008) 51, 495–508 DOI:10.1017/S0013091506000988

Thingstad, T. Frede and Risto Lignell 1997. Theoretical models for the control of bacterial growth rate, abundance, diversity and carbon demand. Aquatic Microbial Ecology. 13:19–27

Thingstad, T. Frede 2000. Elements of a theory for the mechanisms controlling abundance, diversity, and biogeochemical role of lytic bacterial viruses in aquatic systems. Limnol. Oceanogr., 45(6), 2000, 1320–1328

Torres-Barceló, Clara ., Paul E Turner, Angus Buckling, 2022 Mitigation of evolved bacterial resistance to phage therapy, Current Opinion in Virology, 53:101201, https://doi.org/10.1016/j.coviro.2022.101201.

Trinh J. T., Székely T.,, Shao Q., Balázsi G., & Zeng L. 2017. Cell fate decisions emerge as phages cooperate or compete inside their host. Nature Communications 8:14341, DOI: 10.1038/ncomms14341

Tsao YF, Taylor VL, Kala S, Bondy-Denomy J, Khan AN, Bona D, Cattoir V, Lory S, Davidson AR, Maxwell KL. 2018. Phage morons play an important role in pseudomonas aeruginosa phenotypes. J Bacteriol 200:e00189-18. https://doi.org/10.1128/JB.00189-18.

Van Belleghem JD, Dabrowska K, Vaneechoutte M, Barr JJ, Bollyky PL. 2019 Interactions between Bacteriophage, Bacteria, and the Mammalian Immune System. Viruses. 2019; 11(1):10. https://doi.org/10.3390/v11010010

Vallenet D, Nordmann P, Barbe V, Poirel L, Mangenot S, Bataille E, Dossat C, Gas S, Kreimeyer A, Lenoble P, Oztas S, Poulain J, Segurens B, Robert C, Abergel C, Claverie JM, Raoult

D, Medigue C, Weissenbach J, Cruveiller S. 2008. Comparative analysis of Acinetobacters: three genomes for three lifestyles. PLoS One 3:e1805. https://doi.org/10.1371/journal.pone.0001805.

Vega Thurber, Rebecca L., Katie L. Barotta, Dana Halla, Hong Liua, Beltran Rodriguez-Muellera, Christelle Desnues, Robert A. Edwards, Matthew Haynesa, Florent E. Anglya, Linda Wegleya, and Forest L. Rohwer. 2008. Metagenomic analysis indicates that stressors induce production of herpes-like viruses in the coral *Porites compressa*. Proc. Nat. Acad. Sci. (USA) 105(47) 18413–18418. www.pnas.org/cgi/doi/10.1073/pnas.0808985105

Volterra, V. (1926). Variazioni e fluttuazioni del numero d'individui in specie animali conviventi. Mem. Acad. Lincei Roma. 2: 31–113.

Winter, Christian, Thierry Bouvier, Markus G. Weinbauer, and T. Frede Thingstad 2010. Trade-Offs between Competition and Defense Specialists among Unicellular Planktonic Organisms: the "Killing the Winner" Hypothesis Revisited. Microbiology and Molecular Biology Reviews. Mar. 2010, p. 42–57 doi:10.1128/MMBR.00034-09

Wahida, Adam, Fang Tang, Jeremy J. Barr, 2021 Rethinking phage/bacteria-eukaryotic relationships and their influence on human health, Cell Host & bacteria, Volume 29, Issue 5, 2021,Pages 681–688, ISSN 1931-3128,https://doi.org/10.1016/j.chom.2021.02.007.

Yamauchi, Yohei, Ari Helenius; Virus entry at a glance. 2013. J Cell Sci 15 March 2013; 126 (6): 1289–1295. doi: https://doi.org/10.1242/jcs.119685 0966-842X, https://doi.org/10.1016/j.tim.2018.05.009.

Youle, Merry, Matthew Haynes, and Forest Rohwer 2012, Scratching the Surface of Biology's Dark Matter. Pp. 61–81 in G. Witzany (ed.), Viruses: Essential Agents of Life, DOI 10.1007/978-94-007-4899-6_4.

Zheng, Ronger, Qiqi Wang, Runbiao Wu, Prasad N. Paradkar, Ary A. Hoffmann and Guan-Hong Wang, 2023. Holobiont perspectives on tripartite interactions among microbiota, mosquitoes, and pathogens. The ISME Journal https://doi.org/10.1038/s41396-023-01436-7

Lytic/Lysogenic Transition as a Life-History Switch

Supplementary Material

Joan Roughgarden[1]

September 8, 2023

Terminology

A virus particle that infects a bacterium is a "bacteriophage" (eats bacteria) or just "phage", for short. A complete virus particle is a "virion"—it has a protein coat that is the "capsid" enclosing its nucleic acid genome.

A "virulent phage" enters a bacterial cell, commandeers its replication machinery and after a "latency period", releases copies of itself into the environment, killing the bacterium. "Lysis", from the Latin word for "a loosening", is the process by which the copies are released. The set of released copies is the "burst", the number of copies within the burst is the "burst size".

A "temperate phage" may either reproduce new virus particles for release into the environment while killing the bacterium *or* may integrate into the bacterium's genome and reproduce jointly with it. In the former case, the virus, like a virulent virus, commandeers the bacterium's replication machinery to produce copies of itself that after a latency period lyse from the bacterium killing it. This sequence is the "lytic pathway." In the later case, the virus integrates into the bacterial genome becoming a "prophage" that replicates along with the bacterial genome as the bacterium reproduces. The bacterium is not killed. A bacterium containing a prophage within it is a "lysogen". This sequence is the "lysogenic" pathway.

Following incorporation into a bacterium's genome, a temperate phage may either remain incorporated as a prophage during subsequent bacterial cell divisions. *Or*, it may become virulent by de-incorporating from the bacterium's genome and proceed to produce new virus particles by lysis into the environment while killing the bacterium it formerly resided in.

A prophage may augment a bacterium whose genome it resides in by providing the bacterium with a novel gene expressed through a process of "lysogen conversion" *i.e.*, the bacterium is converted from lacking a function into expressing a function. Prophages often encode genes called "morons" that are not directly involved in viral replication and can confer a benefit to their bacterial host. Such genes are independent transcriptional units of DNA that are expressed while the phage is in the prophage state. Morons can enhance the virulence of bacteria to their own hosts by supplying phage-encoded toxins.

[1]Hawaii Institute of Marine Biology, University of Hawaii, joaner@hawaii.edu and Department of Biology, Stanford University, rough@stanford.edu, ORCID: https://orcid.org/0000-0002-6360-7964.

Terms in virology are defined relative to experimental protocols that have no ready counterpart in ecology, hindering the translation of terms between these disciplines. Virologists define the "multiplicity of infection" or MOI with a protocol whereby phage are added to bacteria in a medium. The ratio of the number of phage to the number of bacteria initially added to the medium is the MOI. In this paper, $v(t) = V(t)/N(t)$, is the ratio of virus particles, $V(t)$, to bacteria, $N(t)$, in their source pools at time, t. Hence, the MOI roughly corresponds to $v(0)$ in this paper.

A "one-step growth curve" is a curve of viral abundance in continuous time from the time of absorption until the time of lysis. The one-step curve may include information about the abundance of virus both within the bacteria as well as in the media. A "multi-step growth curve" is an experimental iteration of the one-step curve obtained by allowing the experiment to run beyond the first step. In this paper, viral abundance, $V(t)$, and bacterial abundance, $N(t)$, are curves in discrete time and are recorded solely at the end of each latency period, not within the latency period. They refer to abundance in the environmental source pools, not to virus within bacteria during a time step. Furthermore, Gadagkar and Gopinathan (1980) define an "effective multiplicity of infection" as the "mean number of phages adsorbed per infected bacterium". They also define the "effective burst size" as the "mean number of phages liberated per phage adsorbed." In this paper, at each time step, m indexes the number of virus in a bacterium where $b(m)$ is the burst size from a bacterium infected with m virus, and although not used here, $b(m)/m$, would represent the effective burst size.

Campbell Model of Virulent Phage/Bacteria Population Dynamics

In 1961, Allan Campbell proposed a mathematical model for the population dynamics of virulent phage and bacteria. The Campbell model (Campbell 1961) introduced features that have persisted in phage/bacteria models until the present day. The Campbell model is:

$$\frac{dN(t)}{dt} = r\,N(t)\left(1 - \frac{N(t)}{K}\right) - c\,V(t)\,N(t) \tag{S1}$$

$$\frac{dV(t)}{dt} = b\,c\,V(t-\tau)\,N(t-\tau) - c\,V(t)\,N(t) - d\,V(t) \tag{S2}$$

where $N(t)$ is the number of bacteria at time t, $V(t)$ is the number of virus particles at time t, $N(t-\tau)$ is the number of bacteria at time $t-\tau$, $V(t-\tau)$ is the number of virus particles at time $t-\tau$, τ is a time lag, r is the bacterial intrinsic rate of increase, K is the bacterial carrying capacity within its environment, c is the rate of conversion of mass-action collisions between virus particles and bacteria into infections, b is the burst size, and d is the per capita disintegration rate of virus particles. (The Campbell model was originally written for a phage/bacteria system in a chemostat. Here the chemostat nutrient flow terms are omitted.)

The Campbell model is a pair of nonlinear delay-differential equations. The first term of Eq. S1 assumes the bacteria grow logistically in the absence of virus. The second term is the loss of bacteria from infection brought about by mass-action random collision of bacteria with virus particles. The first term in Eq. S2 is the production of new virus particles that depend on the collisions that took place τ units of time previously. The time lag, τ, called the latency, is the time needed for the infecting virus particles to manufacture and release new virus particles using the bacteria's nucleotide replication machinery. The next term indicates the loss of free virus particles from the infections taking place at the present time, t. Thus, the virus particles disappear for the duration of the latency period. After infecting bacteria at time $t - \tau$ they reappear at time t as newly minted virus particles.

The Campbell model treats the bacteria and virus as *two* separate populations. This type of model is distinguished from those used in epidemiology that pertain to a *single* population containing multiple classes (Kermack and McKendrick 1927, Anderson and May 1979, Keeling and Rohani 2008, Diekmann *et al*. 2013, Bjørnstad 2018.) The time units in single-population models pertain to the time course of the disease in the host, say days to months, whereas the time units in the Campbell model relate to the kinetics of bacterial and viral replication, say minutes. Some models have been proposed for marine virus and also for bacteria in chemostats that are hybrids between the Campbell-type population model and an epidemiology type model (Beretta and Kuang 1998, 2001, Bull *et al*. 2006).

Equilibrium Coexistence of Virus and Bacteria

The equilibrium point of virus-bacteria coexistence in the Campbell model, $(\hat{N}, \hat{V})$, is found by setting $dN(t)/dt = 0$, $dV(t)/dt = 0$, $\hat{N} = N(t) = N(t-\tau)$, and $\hat{V} = V(t) = V(t-\tau)$ in Eqs. 1 and 2 from the main text yielding

$$\hat{N} = \frac{d}{(b-1)\,c} \tag{S3}$$

$$\hat{V} = \frac{r\big((b-1)\,c\,K - d\big)}{(b-1)\,c^2\,K} \tag{S4}$$

The equilibrium point is independent of the latency time, τ, although τ does influence the stability of the equilibrium. The condition for a feasible equilibrium point of coexistence between virus and microbe is read off from the numerator of Eq. S2 as

$$(b-1)\,c\,K > d \tag{S5}$$

This condition means the birth of virus has to exceed the death of virus. This condition can always be satisfied if K is large enough. Specifically, the bacterial carrying capacity, K, must exceed

$$K_{\text{min}} = \frac{d}{(b-1)\,c} \tag{S6}$$

Table S1: Example Parameters in Campbell Model

r	0.0347
K	10^8
τ	15
b	40
c	10^{-4}
d	0.693

for the virus and bacterial populations to have positive equilibrium values. In fact, K_{min} works out to be the same as $\hat{N}$. Therefore, K must merely be greater than the bacterial abundance expected in the presence of the virus for the equilibrium in Eqs. S1 and S2 to be positive. The $\hat{N}$ is independent of r and K, indicating that its abundance is controlled by the virus' parameters. The $\hat{V}$ does depend on r and K, and increases with the bacteria's r and decreases with the bacteria's K. This dependence of the bacterial abundance on the properties of the virus and of virus abundance on properties of the bacteria is a well known property of Volterra-style predator-prey models in ecology (*c.f.* Roughgarden, 1998, p. 266 *ff*).

Parameters for Campbell Model

Order-of-magnitude guesses at parameter values for the model may be constructed from the literature. Consider the parameters for bacterial logistic growth, r and K. In the laboratory, the doubling time of *E. coli* is 20 minutes although it can be much slower in the wild (Gibson *et. al.* 2018). Assuming time units of minutes, this laboratory doubling time corresponds to $r = 0.0347$ (*i.e.* $0.0347^{20} = 2.00$). Next, in the human gut, which is the habitat of *E. coli*, this bacterium is typically present in 10^6 colony forming units per gram of stool (Foster-Nyarko and Pallen 2022). A typical value for the amount of faeces in a human is one lb or 450 grams (Alexa Answers, Amazon, retrieved July 21, 2022). So, a possible value for K is 10^8.

The time between the viral adsorption and first appearance of viral progeny is 10–15 minutes (Endy *et al.* 1997, Purohit *et al.* 2005). So, a possible value for the latency, τ, is 15 minutes.

The burst size from microbes infected with about two virus is about 80 virus particles (Gadagkar and Gopinathan 1980, Figure 4), so b will be taken as 40.

About one in 10^3–10^4 collisions between a virus and bacterium lead to a specific binding between the cellular receptor and the virus attachment protein on the surface of the virus (Philipson 1983). So in the model c is taken as 10^{-4}.

The half-life of free infectious influenza A virus is ≈ 3 hours (Baccam et al 2006). If the half life is taken on the order of 1 hour, the disintegration rate of free virus, d, works out to be about 0.693 (*i.e.* $d = -\ln(1/2)$).

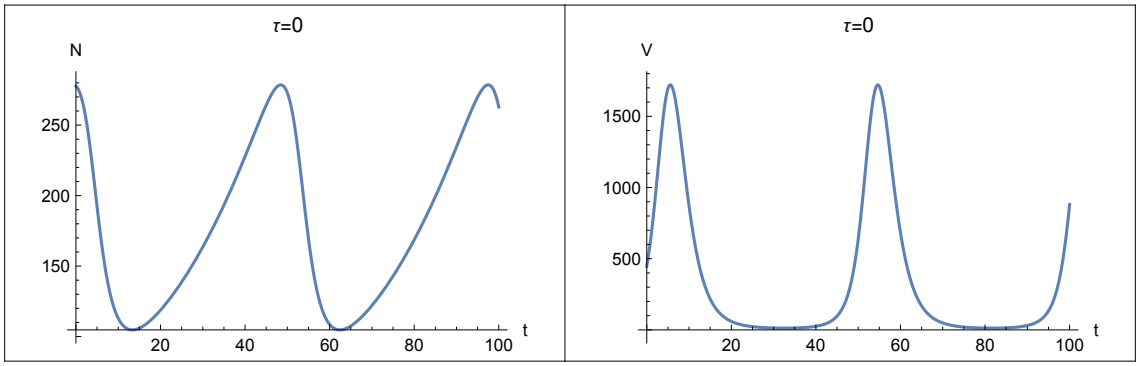

Figure S1: *Virus-Bacteria oscillation from the Campbell model with parameters from Table S1 excepting* $\tau = 0$. *Left is number of bacteria* vs. *time and right is number of virus* vs. *time. Initial conditions are* $N(0) = \hat{N} + 100$ *and* $V(0) = \hat{V} + 100$. *The period of the oscillation is about 55 minutes. Integration is from t = 0 to 100 minutes.*

These guesses at plausible parameter values are summarized in Table S1.

Guesses at plausible parameter values are summarized in Table S1. Using these parameters, the equilibrium from Eqs. S1 and S2 at which bacteria and virulent virus coexist out to be

$$\hat{N} = 177.692 \tag{S7}$$

$$\hat{V} = 346.999 \tag{S8}$$

Stability of Equilibrium with No Latency, $\tau = 0$

The coexistence of bacteria and a virulent virus require both that the equilibrium solutions for $\hat{n}$ and $\hat{v}$ from Eqs. S1 and S2 be positive *and* that the equilibrium point be stable to perturbations.

To begin, assume that the latency, τ, is 0, indicating an instantaneous conversion of virus infections into newly released virus particles. This assumption converts the Campbell model from a pair of delay-differential equations into a pair of Volterra-style ordinary differential equations that can be analyzed with conventional methods. The details of the analysis are recorded in the Supplementary Material.

With $\tau = 0$, the equilibrium is always stable. The trajectories reveal a virus-bacteria oscillation through time that winds in to the equilibrium point. The period of the oscillation is determined by d and r, independent of b, c and K. The oscillation speeds up as d and/or r are increased. A high K diminishes the stability of the virus-bacterial equilibrium point.

The Campbell model, Eqs. 1 and 2, with $\tau = 0$ can be integrated with the NDSolve[] function in *Mathematica*. The solutions appear in the time domain as a nearly endless virus-bacteria oscillation as illustrated in Figure S1 and in a parametric plot as a nested set of loops, each representing a different initial condition, as illustrated in Figure S2. If the bacterial carrying

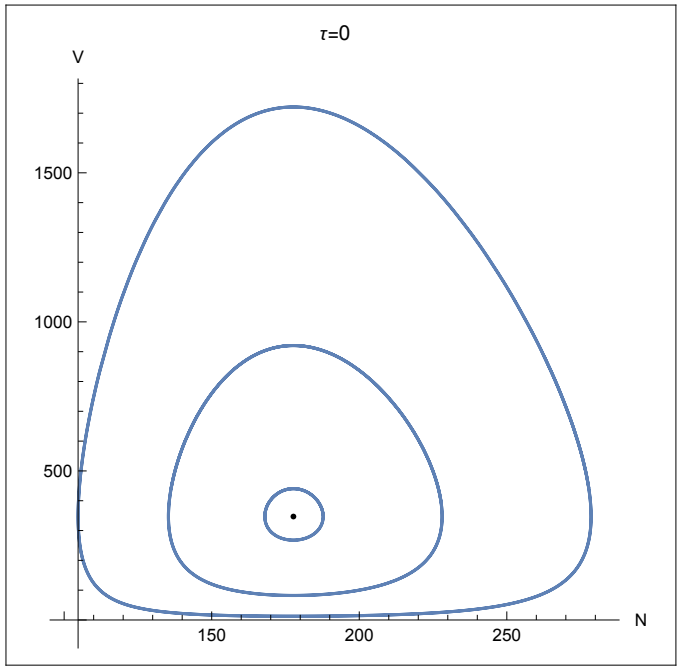

Figure S2: *Parametric plot of the Campbell model with parameters from Table S1 excepting* $\tau = 0$*. Horizontal axis is number of bacteria, vertical axis is number of virus, dot in center is the equilibrium point,* $(\hat{N}, \hat{V})$*. Outer loop was started at* $(N(0) = \hat{N} + 100,\ V(0) = \hat{V} + 100)$*, middle loop started at* $(N(0) = \hat{N} + 50,\ V(0) = \hat{V} + 50)$*, and inner loop started at* $(N(0) = \hat{N} + 10,\ V(0) = \hat{V} + 10)$*. Integration is from t = 0 to 100 minutes.*

capacity within the host is arbitrary set lower than 10^8, say approaching $K_{\min}$ from Eq. S4, then the equilibrium becomes increasingly stable and the trajectories more rapidly spiral into the equilibrium point (not illustrated).

Stability Analysis of Campbell Model with $\tau = 0$

The Jacobian matrix, J, with $\tau = 0$ evaluated at the equilibrium yields

$$J = \begin{pmatrix} \frac{-d\,r}{c\,K\,(b-1)} & -\frac{d}{b-1} \\ r\left(b - \frac{d}{c\,K} - 1\right) & 0 \end{pmatrix} \tag{S9}$$

The eigenvalues of J, λ_1 and λ_2 are a pair of conjugate complex numbers the real part of which is

$$\Re(\lambda) = -\frac{d\,r}{2\,(b-1)\,c\,K} \tag{S10}$$

Because $\Re(\lambda)$ is always negative, the equilibrium is always stable. And because the eigenvalues are complex, the trajectories reveal a virus-bacteria oscillation through time that winds in to the

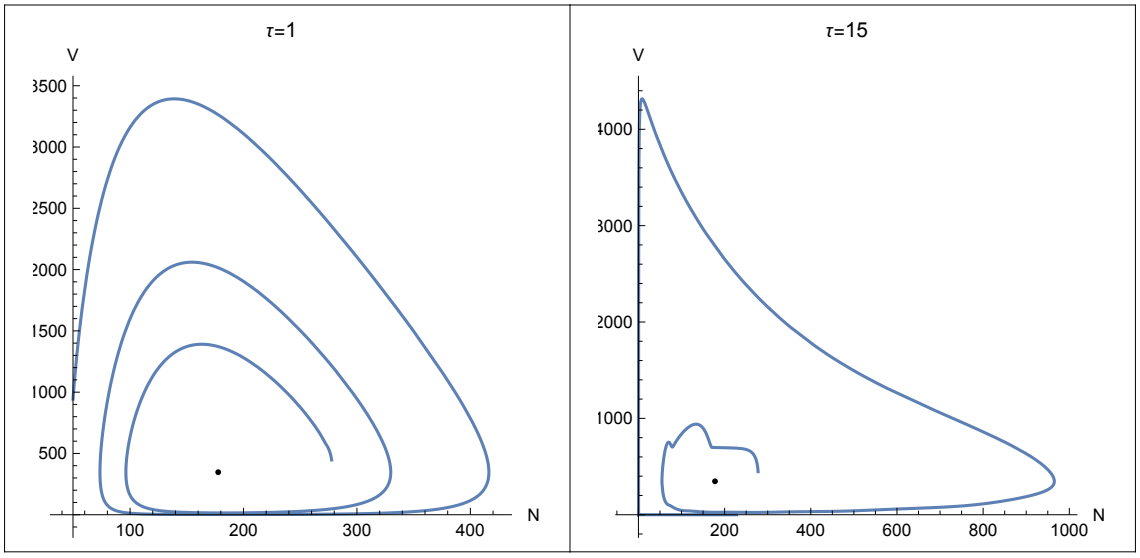

Figure S3: *Left: Parametric plot of the Campbell model with parameters from Table S1 excepting latency, $\tau = 1$ minute. Right: Parametric plot of the Campbell model with parameters from Table S1. Horizontal axis is number of bacteria, vertical axis is number of virus, dot in center is the equilibrium point, $(\hat{N}, \hat{V})$. Initial condition is $(N(0) = \hat{N} + 100,\ V(0) = \hat{V} + 100)$. Integration is from t = 0 to 150 minutes on the left and to 400 minutes on the right.*

equilibrium point in a flow pattern representing a "stable focus". The period of the oscillation is approximately

$$T = \frac{e\,\pi}{\sqrt{d\,r}} \tag{S11}$$

The period is determined by d and r, independent of b, c and K. The oscillation speeds up as d and/or r are increased.

Even though $\Re(\lambda)$ is always negative, its magnitude varies inversely with the bacterial carrying capacity, K. Hence, a high K diminishes the stability of the virus-bacterial equilibrium point. Indeed, if K is infinite, the equilibrium point is neutrally stable and the flow of trajectories represents a "center" as occurs in the original Volterra predator-prey model (Volterra 1926; for a summary *cf.* https://en.wikipedia.org/wiki/Lotka–Volterra_equations, retrieved July 28, 2022).

With the parameters of Table S1,

$$\Re(\lambda) = -3.08 \times 10^{-8} \tag{S12}$$

$$T = 55.07 \text{ minutes} \tag{S13}$$

The $\Re(\lambda)$ for these eigenvalues is nearly zero because k is 10^8 in Table S1 and thus the equilibrium is, practically speaking, neutrally stable.

Stability of Equilibrium with Latency, $\tau > 0$.

The introduction of the latency time lag, τ, destabilizes the equilibrium at which virus and bacteria coexist. Although stability conditions for a system of delay-differential equations cannot generally be analyzed mathematically, the NDSolve[] function in *Mathematica* can successfully numerically integrate the Campbell model with a fixed time lag, τ. The left side of Figure S3 shows the parametric plot of virus and bacteria through 150 minutes with a small latency, $\tau = 1$ minute. The virus and bacteria populations were started toward the right of the equilibrium point, at $N(0) = \hat{N} + 100$ and $V(0) = \hat{V} + 100$, respectively. The trajectories wind out from the initial condition, spiraling ever farther from the equilibrium point.

The dynamic instability caused by the latency period becomes even worse with the realistic latency period of $\tau = 15$ minutes, as was recorded in Table S1. The right side of Figure S3 shows the parametric plot of virus and bacteria through 400 minutes for a 15 minute latency. The virus and bacteria populations were again started toward the right of the equilibrium point, at $N(0) = \hat{N} + 100$ and $V(0) = \hat{V} + 100$, respectively. The trajectories show a jagged start because the initial condition for a delay-differential equation should specify the value of the variables at time $t = 0$ *and* at all times in the past until $t = -\tau$. Because the value of the variable is unknown before $t = 0$, the value at $t = 0$ is attributed to the earlier times. After a while, the trajectory catches up with its history and the trajectory smooths out. Thereafter the trajectories wind out and quickly hug the axes.

Campbell in 1961 may not have been aware of the destabilizing role of the viral latency period. At that time he wrote "If a virulent phage and a susceptible bacterium are mixed in an open growth system, such as a chemostat, one expects that, in general, the concentration of the two will approach some stable steady state value." (Campbell 1961, p157–8). But twenty years later, in 1981, he wrote that "Stable coexistence of phage and bacteria in chemostats has been verified experimentally. Comparison of theory with experiment revealed one discrepancy: Although the concentrations of bacteria and phage stabilized at approximately the predicted values, theoretical analysis and computer simulations predicted unstable oscillation rather than a stable steady state." (Campbell 1981, p. 61). Indeed, researchers testing a version of the Campbell model with chemostats in 1977 wrote, "the time lag due to the latent period of the phage has a destabilizing effect which may be stronger than the opposite, stabilizing, effect of [bacterial population] regulation (Levin *et. al*. 1977, p. 11).

Critique of Campbell Model

Fifty-six years after the ground-breaking Campbell (1961) model appeared, Krysiak-Baltyn *et al.* (2017) published an extensive review of models for virulent phage and bacteria. They observed that "The basic model initially suggested by Campbell, and later refined by Levin and colleagues

[Levin *et al*. 1977], has remained in use since first publication. Later studies have mostly made minor adjustments to the existing model to study dynamic behavior." (p. 964) They further observed that "Earlier studies on simple chemostat models indicated that the dynamics of the model are not in good quantitative agreement with experimental data. In particular, the stability of the simulated models is lower than expected, with many exhibiting heavy oscillations and extinction events where stable steady-states exist experimentally." (p. 964) Krysiak-Baltyn *et al.* (2017) conclude that "On a practical level, the usefulness of computational models of bacteria and phages has not yet been established. The simpler chemostat models may first need to become more accurate" (p. 965).

Thus, the Campbell (1961) model suffers quantitative limitations. First, it predicts instabilities to virulent virus/bacteria population dynamics that are contradicted experimentally. Second, the Campbell (1961) is so mathematically challenging that its use is impractical in biology. How to mathematically analyze a system of nonlinear delay-differential equations is an ongoing subject of research in applied mathematics (Tang and Zou 2008, Huang et. al. 2010; indeed many investigators simply put the time lag, τ, equal to zero to evade the problem, converting the delay differential equations into ordinary differential equations). And as discussed in the text of the main document, the qualitative picture provided by the Campbell model is problematic. The Campbell model envisions that virus/bacteria population dynamics involves two counteracting forces—the stabilizing force of density-dependent bacterial population growth and the destabilizing force of time lags arising from the virus latency period. The outcome is a balance of these forces. This qualitative picture might not be accurate.

Density-Dependent Burst Size

Several choices are available for the burst size from a bacterium as a function of the number of virus in it, $b(m)$. The burst size might increase linearly with m so that $b(m) = b_o\, m$ where b_o is the contribution to the overall burst made by a single viral particle (Patel and Rao 1984, Figures 1–2). This case is for no density dependence. Alternatively, $b(m)$ might be a constant, $b(m) = b_o$, indicating that the burst size does not increase for m beyond the initial infection. A constant $b(m)$ indicates strong density dependence and is consistent with surveys reporting that burst sizes are characteristic of various viral taxa (Parada *et al.* 2006, Ranasinghe 2019). Another possibility is to assume $b(m)$ is a convex increasing function of m (Gadagkar and Gopinathan 1980, Figures 4–5). In this case, the burst-size function might be taken as $b(m) = b_o\, m^\alpha$ where α is an exponent between 0 and 1, say 1/2. A final possibility is to allow α to be negative, say $\alpha = -1$, to indicate that burst size varies inversely with the multiplicity of infection, indicating extremely strong density dependence as a response to "superinfection" (Brown and Bidle 2014). All these possible relations between burst size and m may be subsumed by taking $b(m) = b_0\, m^\alpha$

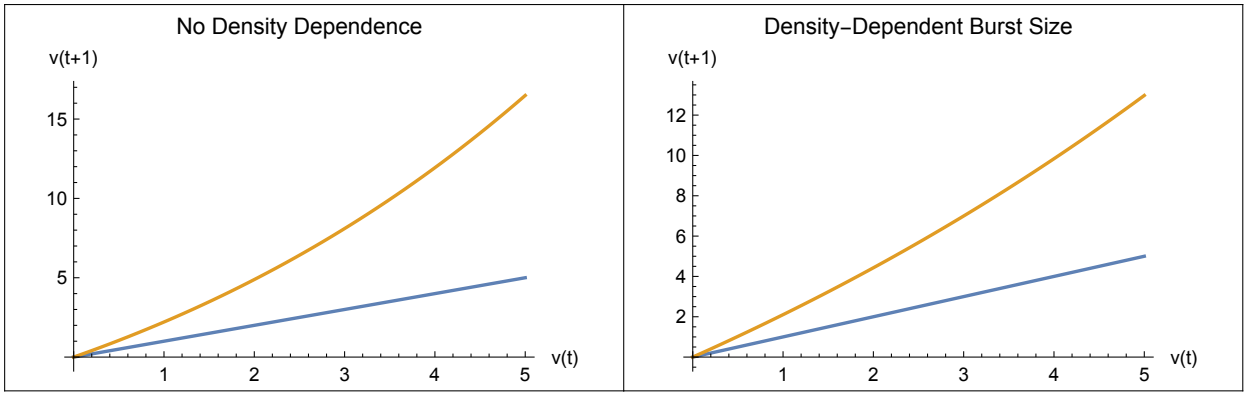

Figure S4: *$v(t+1)$ vs. $v(t)$, in brown, for no density dependence (left) and for a density-dependent burst size (right) from Eqs. 10 and 13, respectively. The diagonal line, in blue, indicates $v(t+1) = v(t)$. An intersection of the brown curve with the blue line would indicate an equilibrium point where virus and bacteria coexist, provided the equilibrium is stable. Because the curve does not intersect the line in either plot, no coexistence occurs in either case. Here, $a_o = 0.1$, $b_o = 40$, and $R = 2$*

with α as 1, 1/2, 0, or -1. Here, the cases of $\alpha = 1$ and $\alpha = 0$ will be investigated analytically. Results (not shown) for other α are similar.

No Density Dependence: $a(v(t)) = a_o$**,** $b(m) = b_o\, m$

Here,

$$\mu(t) = a_o\, v(t) \tag{S14}$$

and, upon doing the summation in Eq. 4 ,

$$\widetilde{b}(\mu(t)) = b_o\, a_o\, v(t) \tag{S15}$$

so Eq. 5 becomes

$$v(t+1) = \frac{b_o}{R}\, \frac{a_o\, v(t)}{e^{-a_o\, v(t)}} \tag{S16}$$

Analysis of this case appears in Figure S4 (Left).

Density-Dependent Burst Size: $a(v(t)) = a_o$**,** $b(m) = b_o$

Here,

$$\mu(t) = a_o\, v(t) \tag{S17}$$

and, upon doing the summation in Eq. 4,

$$\widetilde{b}(\mu(t)) = b_o\, (1 - e^{-a_o\, v(t)}) \tag{S18}$$

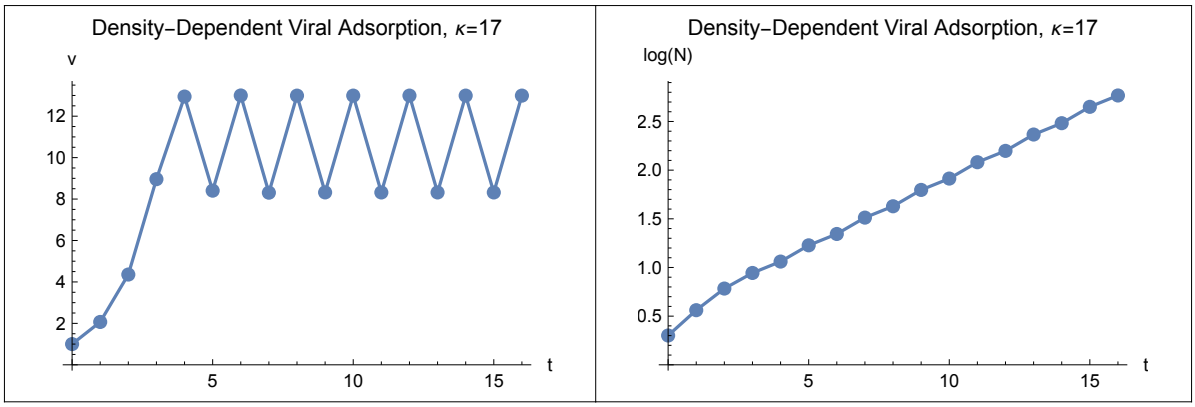

Figure S5: *Left: Trajectory of $v(t)$ showing a two-point limit cycle around the unstable equilibrium at $\hat{v}$. Right: Trajectory of $\log_{10}(N(t))$ showing a two-point oscillation in the exponential bacterial population growth. Here, $\kappa = 17$, $v(0) = 1$, $N(0) = 2$, $t_{\max} = 16$, $\kappa = 12$, $a_o = 0.1$, $b_o = 40$ $R = 2$ and $t_{\max} = 16$.*

so Eq. 5 becomes

$$v(t+1) = \frac{b_o}{R}\,\frac{1 - e^{-a_o\,v(t)}}{e^{-a_o\,v(t)}} \tag{S19}$$

Analysis of this case appears in Figure S4 (Right).

A point of possible coexistence occurs at the value of v for which $v(t+1)$ equals $v(t)$. This condition is shown graphically in Figure S4. An intersection of the curve for $v(t+1)$ with the line for $v(t+1) = v(t)$ would indicate an equilibrium point for possible virus/bacteria coexistence. The curve and line do not intersect in either case. Therefore coexistence, not surprisingly, is impossible without any density dependence, but surprisingly, is also impossible if the density dependence is solely in the burst size assuming the function relating burst size to density is $b(m) = b_0\,m^{\alpha}$. (Illustrated only for $\alpha = 0, 1$.)

Trajectories with $\kappa > 14$

Figure S5 illustrates trajectories of both virus and bacteria for $\kappa > 14$. Trajectories illustrate a two-point limit cycle of $v(t)$ around the unstable $\hat{v}$. The trajectory of $N(t)$ also shows a two-point oscillation around the asymptotic growth factor although again, the scale on the graph makes the oscillations difficult to see.

The existence of a two-point limit cycle around the unstable equilibrium in Figure S5 is consistent with known dynamics for the discrete-time logistic equation (May 1976.) The possibility of more complex oscillations and chaotic trajectories with $\lambda_+ < -1$ remains to be explored. For the purposes of this paper, a comparison of the oscillations for this model in Figure S5 with those in Figures S1–S3 shows that the oscillations in the present model are bounded from above and below whereas those in the Campbell (1961) model approach arbitrarily close to the axes,

implying population extinction.

Poisson Summation Identities

$$\sum_{m=1}^{\infty} P_m(\mu) = 1 - e^{-\mu} \tag{S20}$$

$$\sum_{m=1}^{\infty} m\, P_m(\mu) = \mu \tag{S21}$$